[AMERICAN JOURNAL OF SCIENCE, VOL. 284, DECEMBER, 1984, P. 1125-1174]

THEORETICAL ANALYSIS OF THE ROLE OF GROUNDWATER FLOW IN THE GENESIS OF STRATABOUND ORE DEPOSITS.

2. QUANTITATIVE RESULTS

GRANT GARVEN* and R. ALLAN FREEZE**

Analysis confirms what simple common sense teaches us, namely, the correctness of judgments is as much more probable as the judges are more numerous and more enlightened.

Laplace[1]

ABSTRACT. The role of gravity-driven groundwater flow systems in stratabound ore formation can be studied using numerical solutions of the mathematical models of fluid flow, heat and mass transport, and geochemical reaction paths in two-dimensional cross sections through sedimentary basins. Suites of generic simulations form the theoretical basis of a sensitivity analysis used to evaluate quantitatively the effects of various parameters in the transport models. Most of the simulations are performed on a simple, two-layer, 300-km long, wedge-shaped basin for comparison purposes, but other shapes and sizes are also considered.

The results of the sensitivity analysis indicate that gravity-driven groundwater flow systems are capable of sustaining favorable fluid-flow rates, temperatures, and metal concentrations for ore formation at groundwater-discharge areas near the edge of a basin. Under a gravity-drive mechanism, groundwater flows from recharge areas in the elevated regions of a foreland basin to discharge areas in lower-elevation regions. Flow patterns and rates are largely dependent on the basin geometry, the water-table configuration, and the subsurface variation in permeability. Specific discharge rates on the order of 1 to 10 $m^3/m^2/yr$ are possible in basin aquifers. A gentle topographic slope and continuity in stratigraphy will allow regional flow systems to develop over a scale of several-hundred kilometers. Variations in permeability or perturbations of the surface or basement topography can result in the formation of local flow systems of smaller dimensions. A natural consequence of a gravity-driven flow system is its effect on the thermal regime. Temperatures are depressed in recharge areas and elevated in discharge areas with respect to the thermal gradient due to conduction, because of forced convective heat transport. Depending on the hydrodynamics and thermal parameters, maximum temperatures near the edge of a 300-km long wedge-shaped basin can range from about 50° to 95°C at a depth of less than 1000 m. Temperatures in excess

* Department of Geography & Environmental Engineering and Department of Earth & Planetary Sciences, The Johns Hopkins University, Baltimore, Maryland 21218

** Department of Geological Sciences, The University of British Columbia, Vancouver, British Columbia, Canada V6T 2B4

[1] Laplace, Pierre Simon, *marquis* de, 1749-1827, Théorie analytique des probabilités. Par M. le Marquis de Laplace ... 3. éd. rev. et. augm. par l'auteur: Paris, Mme. Ve. Courcier, 1820.

of 100°C are possible in larger basins. Subsurface layering in a basin causes fluid-flow to be focused across less permeable, metal-rich shale beds into high-permeability carbonate or sandstone aquifers, which allow for the transport of metal-bearing brines to discharge zones at the basin margin. Long-distance transport of metal and sulfide in the same fluid can probably be ruled out largely on hydrogeochemical grounds but also because of the diluting effects of dispersion. The transport of metal in sulfate-bearing brines is a more defensible geochemical model, in which case the presence of reducing agents helps control the location of ore deposition. Hydrodynamic conditions that could result in ore formation through the mixing of chemically-distinct fluids from regional flow systems are rare.

Quantitative modeling of transport processes in a variety of hypothetical cross sections has shown that gravity-driven flow provides a simple yet realistic explanation for the mechanics of epigenetic ore formation in sedimentary basins. The results of this study also infer an additional application to the understanding of other basin-related geologic processes, such as sediment diagenesis and petroleum migration and accumulation.

INTRODUCTION

Epigenetic, stratabound ore deposits form in sedimentary basins as the result of the existence of a fluid-flow system capable of transporting significant quantities of ore-forming constituents to a depositional site. Part 1 of this study (Garven and Freeze, 1984) provided the theoretical framework for the analysis of one possible fluid-flow mechanism: gravity-driven groundwater flow. A two-dimensional mathematical model of a sedimentary basin was constructed, and numerical methods were implemented to solve the equations governing fluid flow, heat transport, and mass transport with water-rock reactions. Output from the computer simulations consists of plotted cross sections of the hydraulic-head distribution, velocity field, temperature pattern, and concentration patterns in the basin, as well as a reaction-path scenario at the ore-forming site.

The purpose of this paper is to carry out a detailed sensitivity analysis with the numerical models. The goal of these experiments is to determine the influence of various factors on the transport processes involved in the formation of stratabound ore deposits. It will be shown that a wide variety of subsurface flow patterns can exist in a sedimentary basin, and that these flow patterns in turn affect heat and mass transport in the subsurface. Simulation of hypothetical basins will demonstrate the nature of gravity-driven fluid-flow systems, the factors affecting fluid-flow rates and patterns, the factors affecting subsurface temperatures, and the factors influencing the composition of metal-bearing brines as they move through a basin.

A sensitivity analysis can take one of two different routes, depending on the purpose of the study. One approach is called *site-specific*, because the modeling is designed for a particular geologic basin or specific ore deposit. It can yield detailed information, provided an adequate amount of data can be collected to calibrate the model. The second approach is known as *generic*, because the simulations are carried out for hypothetical basins. Such models are designed to reflect many of the geologic features observed in real sedimentary basins but are purposely kept simple in order to be of general use in understanding the phenomena being studied. For the generic approach, a range of realistic parameter data is chosen to assess general mechanisms and to assess the sensitivity of the model results to a change in the numerical value of any particular parameter. Generic modeling forms the main basis of the analysis in this study.

The simulation results given below are divided into several sections, as outlined in table 1. First, the factors affecting fluid flow, heat transport, and mass transport are independently and systematically examined. All these simulations are performed in a simple, two-layer basin model. A variety of more complex geologic configurations are also introduced, although the discussion is kept brief. To complete the analysis, several geochemical reaction-path simulations are evaluated, and the results discussed in light of the constraints imposed by the fluid-flow system. The numerical simulations presented in this paper have been selected from a more comprehensive study (Garven, ms). We believe that these examples

TABLE 1

Simulation parameter	Figures
Fluid flow	
Anisotropic hydraulic conductivity	2
Layering	3
Discontinuous layers	4
Temperature- and salinity-dependent flow	5
Basin length	6
Basin thickness	7
Basement structure	8, 9
Water-table configuration	10
Heat transport	
Thermal conductivity	11
Layering	5, 12
Hydraulic conductivity	12, 13
Geothermal flux	14
Basin size	15
Basement structure	16
Water-table configuration	17
Mass transport	
Dispersivity	18
Hydraulic conductivity	19
Transport distance	20
Layering	21
Geochemical transport and reaction paths	
Metal-sulfate brine model	
A. reaction with hydrogen sulfide	22
B. reaction with methane	23
C. reaction with pyrite	24
Metal-sulfide brine model	
A. reaction with dolomite	25
B. effect of cooling	26

are sufficient to demonstrate some important results regarding the role of gravity-driven groundwater flow in stratabound ore genesis.

CONTROLS ON FLUID-FLOW PATTERNS AND FLOW RATES

Tóth (1962, 1963) and Freeze and Witherspoon (1966, 1967, 1968) showed that the most important factors affecting groundwater flow patterns are: (1) depth-to-lateral extent ratio of the basin, (2) topography or water-table configuration, and (3) stratigraphy and the resulting variations in the hydraulic conductivity. In this section, some of these controlling factors are examined in greater detail for large-scale flow in sedimentary basins. Emphasis is placed on demonstrating the role of basin-wide aquifers in directing flow across less permeable beds to focus flow toward discharge areas and on examining temperature and salinity effects not considered by the earlier studies.

As a starting point, consider a cross section through a sedimentary basin of the shape and size depicted by the finite-element mesh shown in figure 1. The region of flow and boundary conditions are based on the same criteria as those listed for the simulation example given in part 1. This mesh is used throughout the sensitivity analysis unless otherwise specified. It consists of 410 triangular elements and 252 nodes. Topographic relief (water-table configuration) varies linearly with a total drop of 1000 m over the 300 km length of the basin. The vertical scale of the plot (fig. 1) is exaggerated by a factor of 10:1 in order to show the simulation results. The true-to-scale diagram of the basin is plotted directly above the mesh to illustrate the nature of the vertical exaggeration.

Hydraulic conductivity.—For fixed fluid properties and a constant hydraulic-head gradient, the magnitude of groundwater flow is solely determined by the hydraulic conductivity of the porous medium. The range of values of hydraulic conductivity of geologic materials is very wide, sometimes exen extending over several orders of magnitude for the same rock type. Table 2 shows the range established for a variety of lithologies, as listed by Freeze and Cherry (1979). Brace (1980) provides an additional source. Porosity is also important in that it is used to

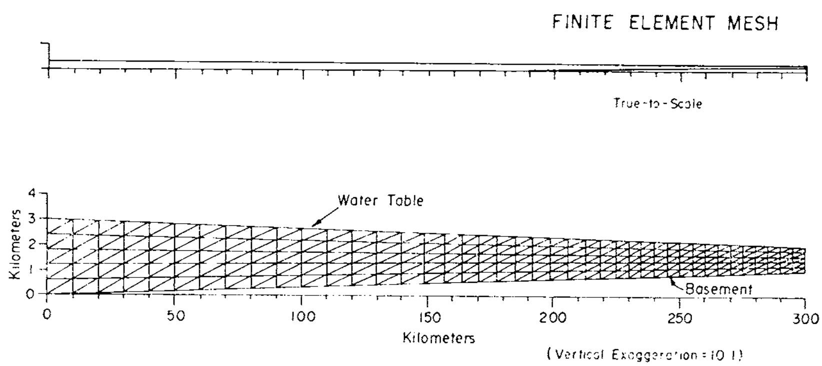

Fig. 1. Finite-element mesh and basin dimensions for sensitivity analysis.

TABLE 2

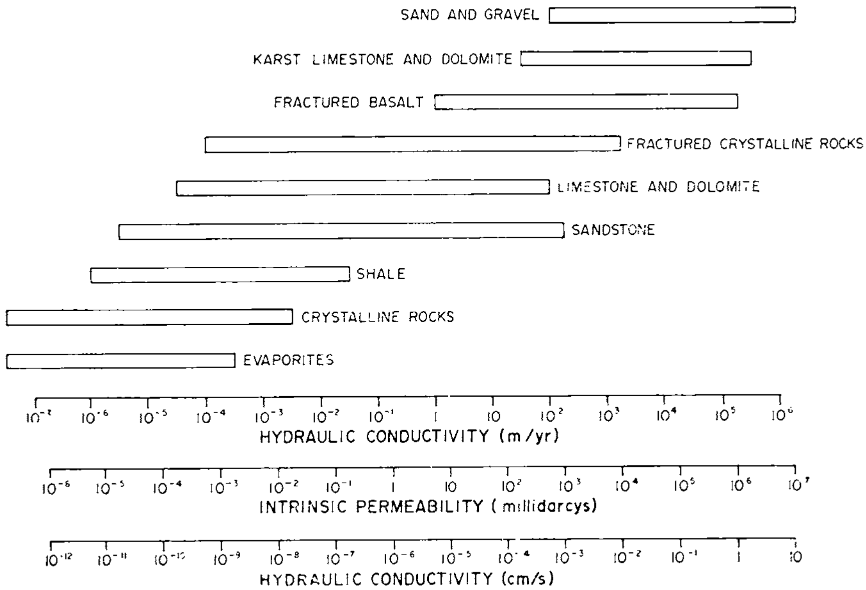

TABLE 3

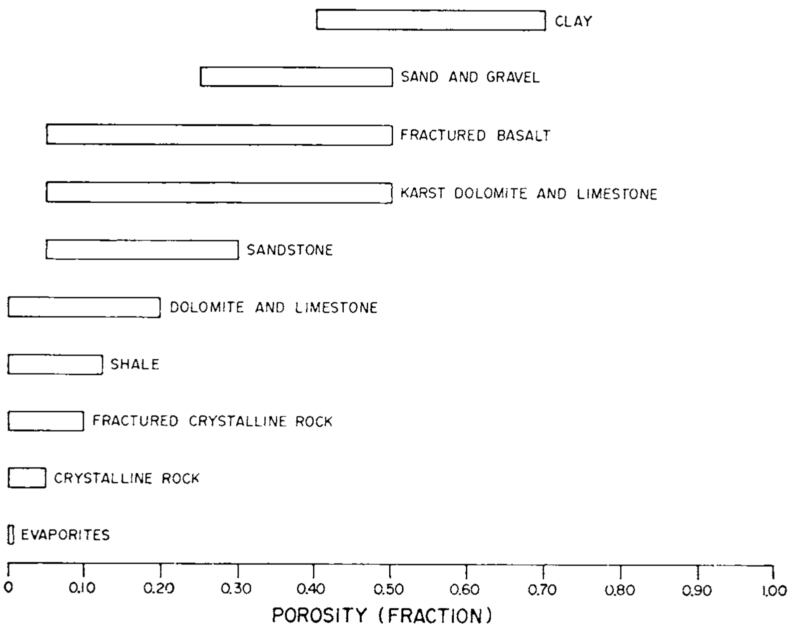

calculate the average linear velocity or seepage velocity of the fluid. Table 3 lists the porosity range of values for the common rock types, which is based on data given by Davis (1969) and Freeze and Cherry (1979).

The simplest hydrogeologic model of a sedimentary basin is the case of a homogeneous and isotropic permeability distribution. Under these conditions in a long, thin basin such as figure 1, the fluid-flow pattern is virtually horizontal and uniform because of the nearly constant hydraulic gradient imposed by the linear slope of the water table (Garven, ms).

Sedimentary rocks are rarely isotropic with respect to the hydraulic conductivity. Figure 2 illustrates the effect of a ratio of horizontal to vertical hydraulic conductivity, K_{xx}/K_{zz}, of 100:1 on the fluid-flow regime in the hypothetical basin model. Anisotropy ratios of this magnitude are commonly encountered in regional groundwater regimes (Freeze and Cherry, 1979), due to the effects of layered heterogeneity, and even higher ratios may be representative when modeling fluid flow in large sedimentary basins. In figure 2, $K_{xx} = 100$ m/yr, $K_{zz} = 1$ m/yr, and the effective porosity is set at a constant value of 0.15. It is assumed for the time being that no salinity or temperature gradients exist in the basin. For this simulation, the components of the average linear velocity are $v_x = 2.3$ m/yr and $v_z = 5.4 \times 10^{-3}$ m/yr at reference point A. The velocity-component ratio depends on the anisotropy ratio of the strata, the point of reference in the basin, and other factors. In a homogeneous cross section with a homogeneous fluid, the magnitude of the velocity vector depends on the value of the porosity. For example, the specific discharge or Darcy velocity at the reference point A (fig. 2) is $q = 0.33$ m^3/m^2 yr. The average linear velocity, however, will be $v = 33$ m/yr, 3.3 m/yr, and 1.65 m/yr for assumed effective porosities of 0.01, 0.10, and 0.20 respectively.

In folded or fractured strata, the principal directions of permeability may not coincide with our x–z axes. Several numerical experiments were run to test the sensitivity of the modeling results to the simple case of dipping strata. The effect of inclining the principal directions of hy-

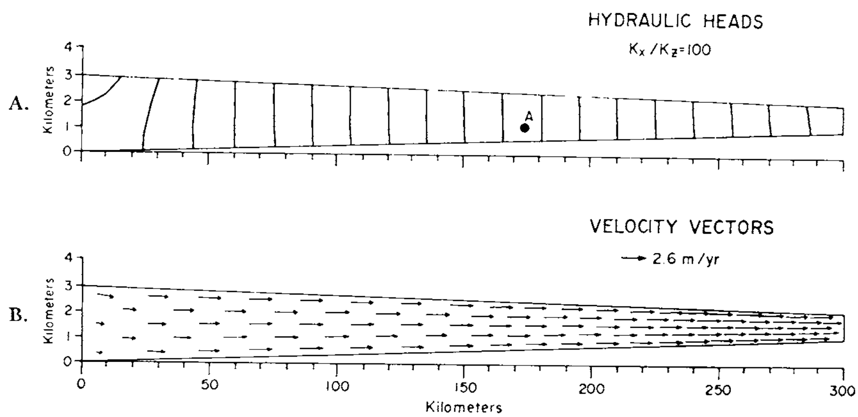

Fig. 2. Effect of anisotropy on fluid flow.

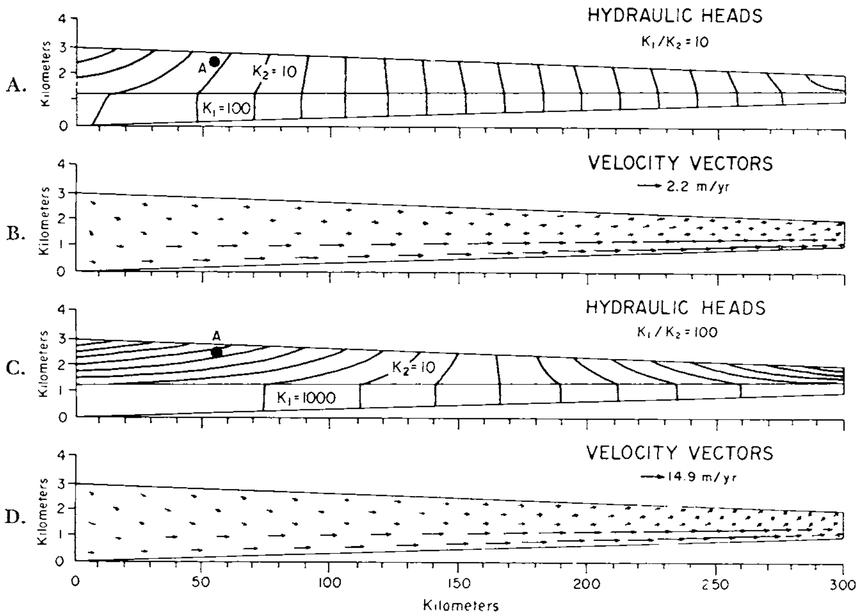

Fig. 3. Effect of layering on fluid flow.

draulic conductivity appears to be negligible for bedding dips of 0.3° or 3m/km (fig. 2). Flow patterns are affected, however, if the beds dip at slopes exceeding 5°. It would be advisable to account for this factor in any studies that consider the formation of ore bodies in structurally complex stratigraphic sequences. For the purposes of this study, only horizontal or gently-dipping strata are further considered.

A layered sedimentary basin is more conducive to focusing of flow than a homogeneous basin. Consider the simple, two-layer model shown in figure 3A. The bottom layer is a carbonate aquifer with a hydraulic conductivity $K_{xx} = 100$ m/yr and a porosity $\phi = 0.15$. The top layer represents a less permeable shale unit, in which $K_{xx} = 10$ m/yr and $\phi = 0.10$. Anisotropy in both layers is assigned a representative ratio of 100:1. Fluid flow is directed down across the shale beds into the carbonate aquifer in the recharge uplands, flows laterally across the basin in the midsection, and is eventually forced up along the discharge end of the basin. Notice that the areas of highest flow are located in the basal aquifer and near the basin margin (fig. 3B). The ratio of the hydraulic conductivity values of the two layers controls the areal extent and degree of vertical flow recharging the basal aquifer. A greater contrast between aquitard and aquifer produces a larger component of vertical flow, which is witnessed by a sharper bending of the hydraulic-head contours (fig. 3C). For example, the velocity ratio v_x/v_z at reference point A in figure 3 changes from 15:1 to 2:1 as the ratio between the layer hydraulic conductivities, K_1/K_2, changes from 10:1 to 100:1. The main qualitative observation to be made here is that the presence of permeability contrasts in gravity-driven flow systems manifests a natural mechanism for the transport of ore-forming constituents from over wide areas of source rocks, with focusing of fluid flow toward more permeable layers.

The effect of discontinuous layers or pinchouts on flow systems is shown by the example in figure 4. The occurrence of a partial basal aquifer in the downstream end of the basin causes a local flow system to develop in this region whereby a recharge area serves to focus flow down into the lens. The expanded picture of the flow field (fig. 4) illustrates a situation where shallow-origin H_2S-bearing waters could continuously recharge into the partial basal aquifer from above, while metal-bearing brines are also recharging the aquifer at the upstream end of the lens.

Other types of layered stratigraphy have been studied with the numerical model. Although many of these are of interest, space does not permit an examination of every case. The basin-wide aquifer model treated above is simple and well-suited for a preliminary analysis of ore genesis. We will proceed, therefore, to examine only the two-layer model in greater detail.

Temperature and salinity gradients.—It was shown in part 1 of this study that the density and viscosity of water are strongly dependent on temperature and salinity over the range of subsurface conditions expected in sedimentary basins.

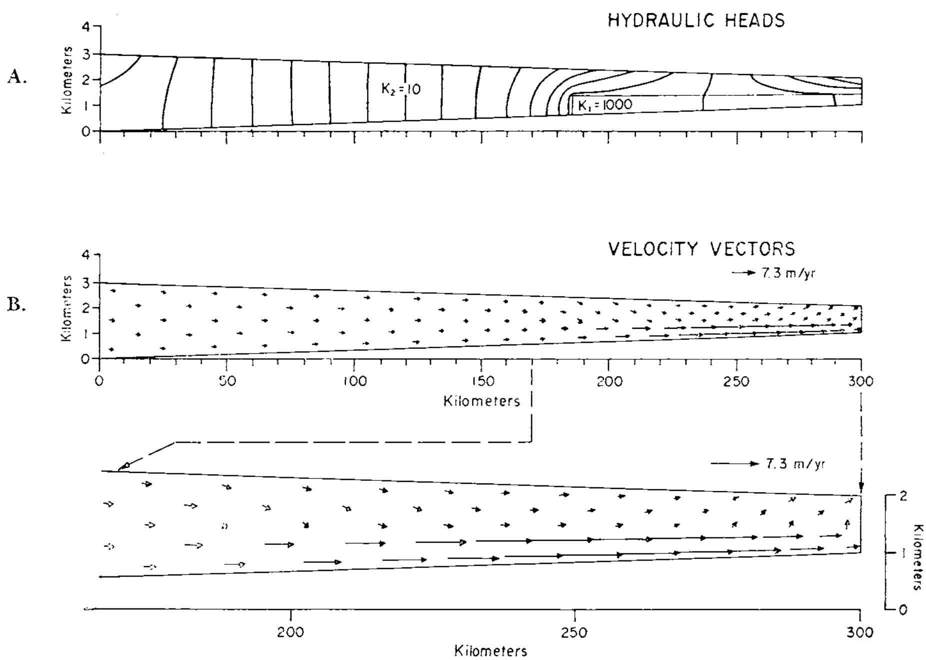

Fig. 4. Effect of aquifer lens in downstream end of basin.

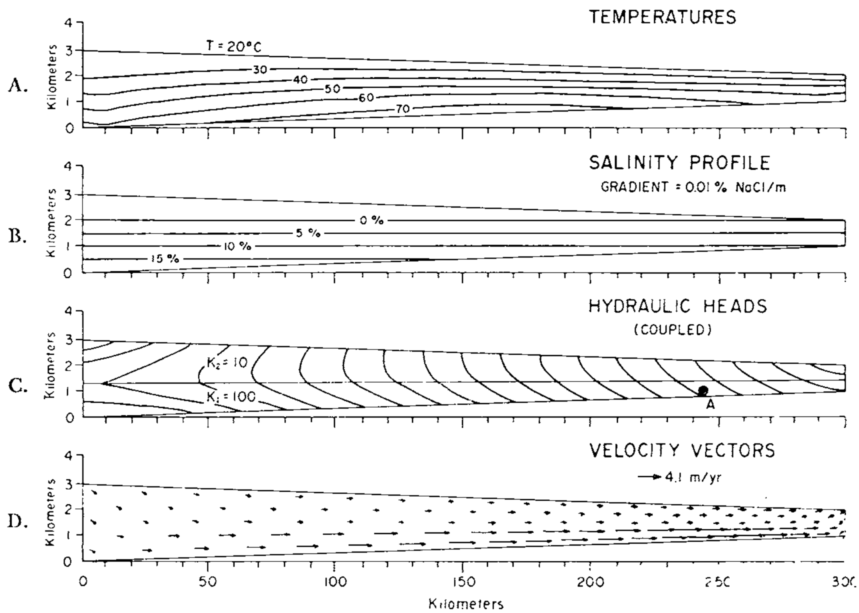

Fig. 5. Effect of combined temperature- and salinity-dependent fluid properties on regional flow system.

A detailed sensitivity analysis was performed using the two-layer basin model of figure 3A in order to determine the quantitative effects of temperature and salinity on the fluid-flow regime (Garven, ms). Figure 5 shows the results of one of these simulations, where both temperature and salinity gradients affect the fluid properties. The hydraulic conductivity of the basal unit is $K_{xx} = 100$ m/yr, whereas that of the upper unit is 10 m/yr. Porosities are 0.15 and 0.10 respectively. Both hydrostratigraphic units have an anisotropy ratio of 100:1. The temperature pattern (fig. 5A) is computed through the numerical solution of the heat-transport equation. The discussion of factors controlling heat flow is reserved for later, and for now we will just present the solution without explanation. Groundwater above the 2000 m elevation level is assumed to be fresh and therefore of zero salinity (fig. 5B). Below this datum, the salinity increases linearly with depth. Salinity is contoured as an equivalent wt percent of sodium chloride, percent NaCl. At the deepest point in the basin, an assumed gradient of 0.01 percent NaCl/m produces a salinity of 20 percent NaCl or about 4.3 molal. The salinity gradient chosen here is arbitrary, yet realistic in range, but field data could easily be inserted in basin-specific simulations.

Comparison of figures 3A and 5C illustrates the main effect of salinity and temperature on the hydraulic-head pattern in the basin. A series of simulations have shown that the buoyancy effect of salinity-dependent density is the primary cause for the modified head pattern (Garven, ms). It should be pointed out that one can no longer use the rule whereby flow vectors are drawn perpendicular to hydraulic-head contours when modeling inhomogeneous fluid flow. For the case of inhomogeneous fluids, the hydraulic head represents a fresh-water equivalent pressure head, not a true hydraulic potential. However, contoured hydraulic-head sections are still useful for comparison purposes.

The influence of temperature and salinity on flow can also be seen through a comparison of velocity profiles. The horizontal component of the average linear velocity at the reference site A (fig. 5C, D) is 3.8 m/yr in the salinity- and temperature-dependent flow problem but only 2.2 m/yr in the uncoupled flow problem (fig. 3A, B). For the case of temperature-dependent flow only, the velocity at this reference site is 4.7 m/yr (Garven, ms). If only the salinity gradient existed, the flow velocity reduces to 1.8 m/yr, and upward components of flow are reduced slightly.

Several simulations were also made using other salinity gradients, with a range from 0 to 0.020 percent NaCl/m. The largest gradient gives a salinity of about 25 percent NaCl and a velocity of 2.8 m/yr at reference point A. We will employ the 0.01 percent NaCl/m gradient in the simulations to follow as being a representative value for the basin model.

Basin geometry.—Fluid-flow simulations can also be conducted to investigate the influence of basin size, structure, and topography on groundwater flow systems. In the preceding simulations the size of the basin was kept a constant 300 km in length and 3 km thick (at the thickest point of the wedge). It is obvious that basin size will vary: some flow systems may operate over distances of only a few kilometers, whereas others may involve distances of several hundred kilometers. Tóth (1963) and Freeze and Witherspoon (1967) demonstrated with their models that the total continuous length of a regional flow system depends on topographic relief, basin thickness, and subsurface permeabilities. If the basin is reasonably thick, relief is gentle, and aquifers exist at depth, then continuous flow systems will develop on a basin-wide scale (figs. 1-5). Numerous field studies have documented the existence of long, gravity-type flow systems in sedimentary basins (van Everdingen, 1968; Hitchon, 1969a, 1969b; Bond, 1972; and Tóth, 1978).

The effect of basin size on subsurface flow is largely controlled by the relative geometry of the basin dimensions. In the case of homogeneous fluid flow (that is, no temperature and salinity gradients present), one can invoke the mathematical concept of dimensional similitude to study the effect of basin size. The similitude concept recognizes that for similar ratios of controlling parameters, such as topography, permeability, and length-to-depth ratio, the quantitative results are similar. Basin similitude, therefore, allows one to extrapolate modeling results to different system scales under these criteria. For example, the flow pattern in figure 3A would be exactly the same in a basin 150 km long by 1.5 km thick or a basin 30 km long by 300 m thick, given the same shape and same hydraulic parameters, because the length-to-depth ratio $L/D = 100$ for all three cases. In figure 6 hydraulic-head patterns are illustrated for two-layer basins of constant thickness of 3 km but with varying lateral extents. Halving the basin length from 300 to 150 km (fig. 6B) and doubling the water-table slope causes increases in fluid velocities throughout the basin, especially in the vertical direction. If the basin length is shortened by a factor of ten (fig. 6A), a considerable amount of energy is required to force fluid flow to the same depth but over a shorter length. As a result, the hydraulic-head equipotentials exhibit large gradients in the upper, low permeability unit and very low gradients in the basal, high permeability unit. Basins with small length-to-depth ratios will be effective at producing large vertical fluxes over broad areas, but, unless high topographic relief exists, flow rates will be significantly smaller than those basins with larger L/D ratios.

Changing the thickness of a basin of constant length produces similar results (Garven, ms). The thicker the basin, the steeper the hydraulic-head gradient becomes in the low permeability unit. Figure 7 summarizes the relationship between the average linear velocity at reference site A (fig.

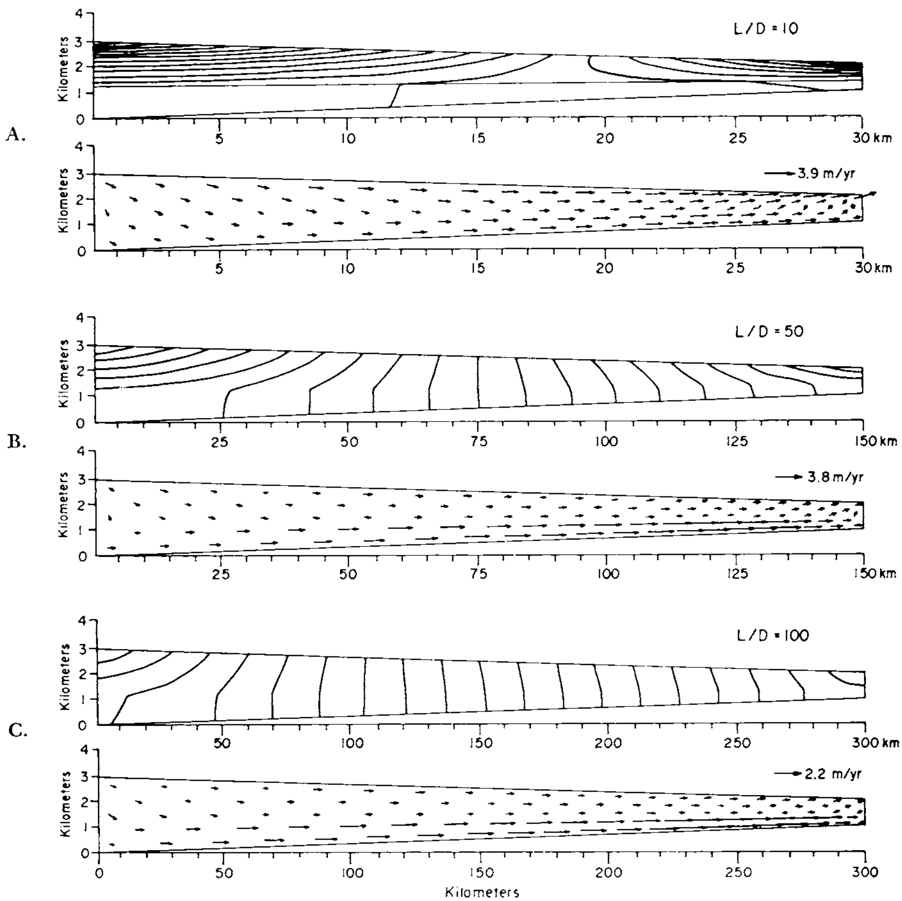

Fig. 6. Hydraulic-head patterns as a function of the length-to-depth ratio (L/D) of a 3 km-thick basin.

5C), basin thickness, and topographic gradient. Most of the velocity change is created by the changing water-table slope. Qualitatively, it may prove useful in future studies to consider a suite of steady-state models in assessing the change in flow patterns as a basin evolves through geologic time.

Basement structure also affects flow patterns in a basin. The sloping-basement structure assumed in the preceding models was designed to characterize a basal flow boundary with gentle relief. In many sedimentary basins, this flow boundary can be suitably placed at the unconformity with the crystalline, Precambrian basement. With the numerical model, many types of simulations can be performed to study the effect on the flow field of other types of basement structures (Garven, ms). As an example, figure 8 considers the situation where an extensive arch occurs along a gently-dipping basement. The presence of this basement ridge causes flow to be focused up over the ridge, with some discharge to the land surface above the structure.

Figure 9 summarizes the influence of basement structure on fluid dynamics for three distinct cases: (1) flat-bottom basin, (2) sloping-bottom

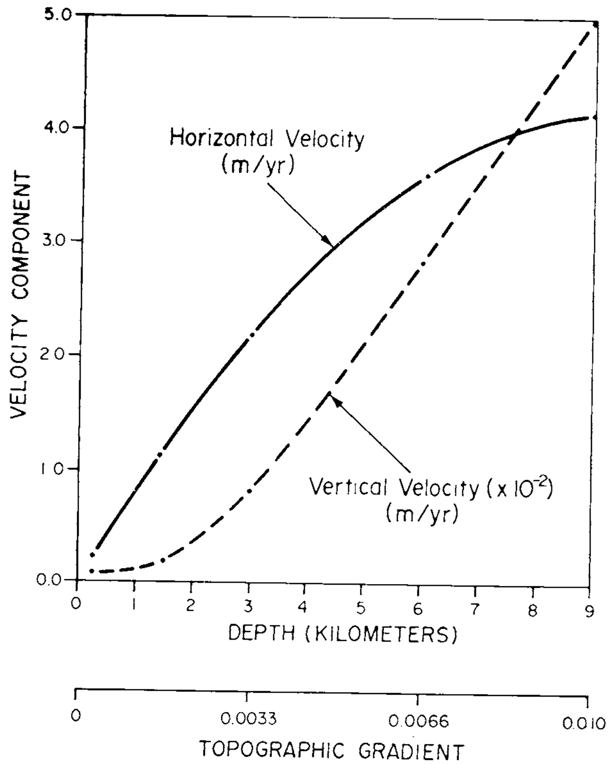

Fig. 7. Average linear velocity components as a function of basin depth and topographic gradient, for reference point A in the downstream end of the basin (see fig. 8A).

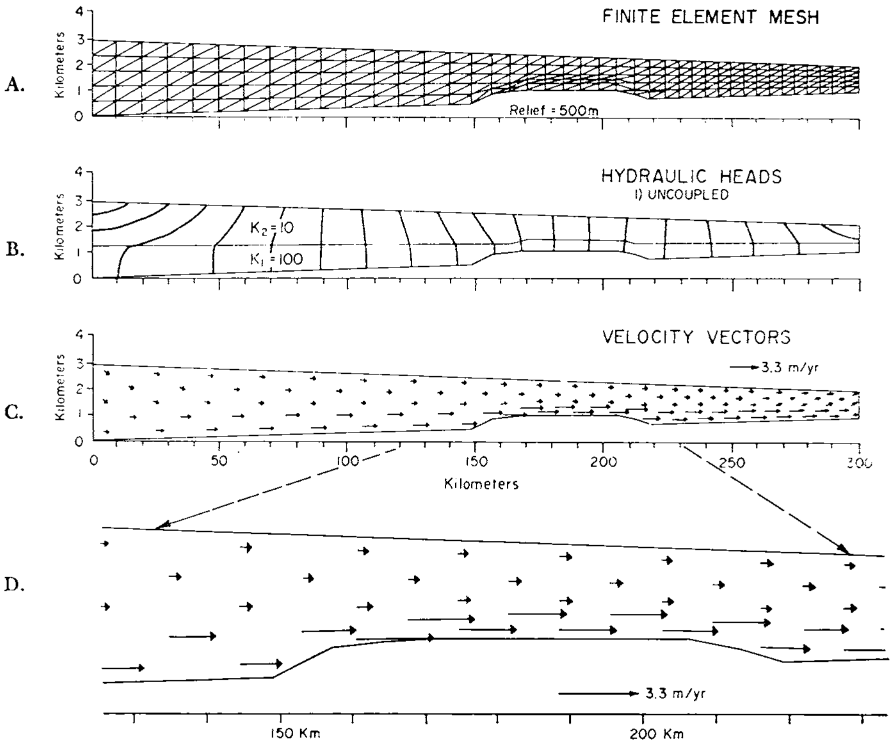

Fig. 8. Regional fluid-flow patterns in a basin containing a basement arch with a relief of 500 m.

basin, and (3) sloping-bottom basin with basement arches. The latter case is documented for basement ridges with reliefs of 500 and 1000 m over the regional dip. The average linear velocity distribution in the basal hydrostratigraphic unit of each case is plotted as a function of distance along the x axis. For comparison purposes, all four simulations assume there are no temperature or salinity gradients in the basin. The velocity distribution becomes quite complicated when the impermeable bottom surface is perturbed by a basement high. Horizontal flow rates increase over the ridge structure, and upward vertical gradients (fig. 8D) are introduced. Phenomena of this type could be important in explaining the genetic association of stratabound ore deposits and basement highs. The conceptual effect of the basement-arch structure has been recognized by geologists for a long time — the results given here quantitatively confirm its effect.

Water-table configuration.—The mechanism responsible for driving a gravity-based flow system is the water-table gradient. Recall that by definition the water table is an imaginary surface below ground level at which gage pressure is zero. The water table is also the upper boundary of the saturated flow field, which in this study is assumed to be a subdued replica of the topography. As we have shown, the slope of the water table is a major factor in determining hydraulic-head gradients in the subsurface and therefore flow rates (fig. 7). Similarly, it should come as no surprise that the configuration of the water table exerts a strong control on the geometry of flow systems in basins. The influence of this factor has been documented for fresh-water, isothermal basins by Tóth (1963) and Freeze and Witherspoon (1967) and for variable-fluid density and non-isothermal sedimentary basins by Garven (ms). Based on these studies it is clear that a constant and gentle regional slope produces a long continuous flow system across a basin, whereas the existence of a rugged and irregular water-table configuration results in the development of various local flow systems, which superimpose their effects on the regional system.

One might expect that as a sedimentary basin begins to be uplifted and epeiric seas regress from the region continuous flow systems would operate across the basin and do so for long periods of geologic time. Presumably, this type of flow regime is conducive to ore-forming processes occurring near the edge of a basin as metal-bearing brines are discharged in this area. Depending on the character of surface drainage, the rates of erosion and tectonic history, regional flow systems will eventually experience some form of perturbation as major ridges or valleys develop. The result of a major discharge area will be the focusing of flow to this area, which thereby places constraints on the location of ore formation. If the

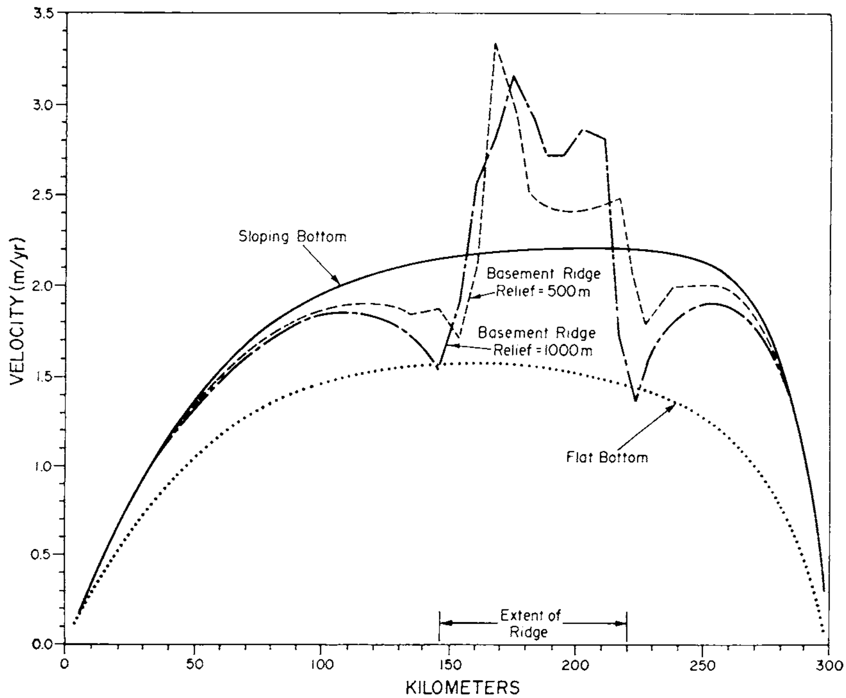

Fig. 9. Effect of basement structure on the fluid velocity in a basal aquifer.

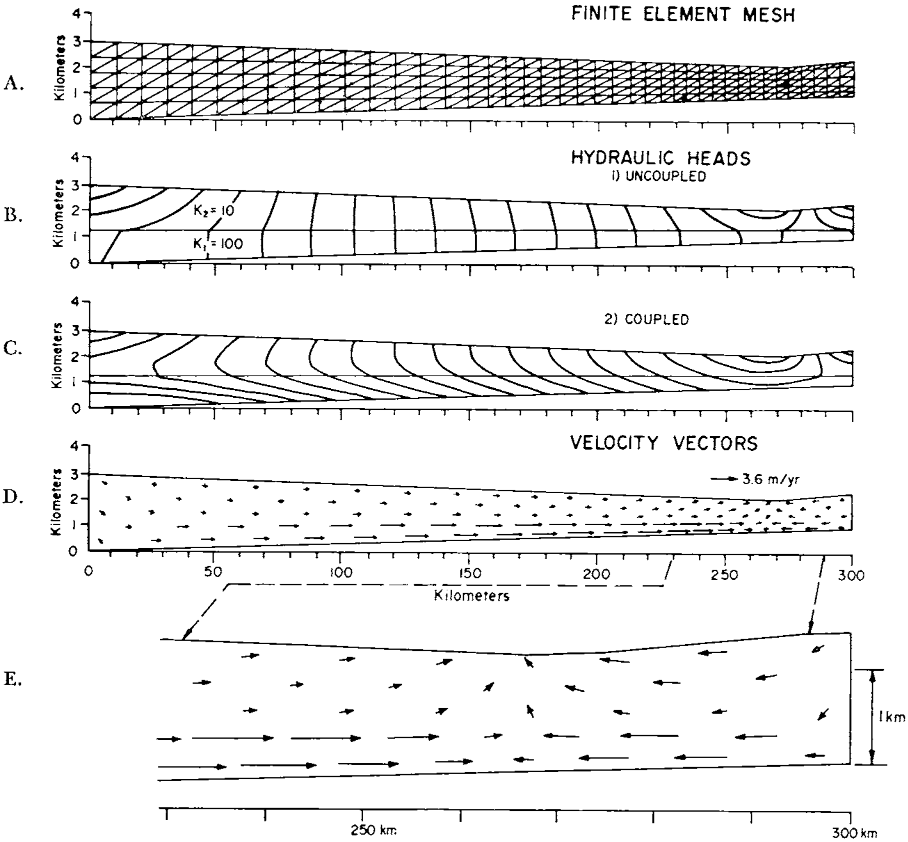

Fig. 10. Regional fluid flow with a water-table rise at the basin margin.

water-table were to become very rugged, it is possible that no ore deposits may form because of the strong influence of local flow systems in disrupting the flow of warm brines from deeper parts of the basin.

An example of the effect of the water-table configuration on subsurface flow patterns is given in figure 10. The model assumes a simple, two-layer hydrostratigraphy with the same material properties as those used in preceding simulations (fig. 5). Temperature and salinity effects are included in this simulation example. The presence of a rise in the topography at the margin of the basin causes a local flow system to appear, which is directed against the regional system, and it forms a groundwater-flow divide at the foot of the rise (fig. 10). The ridge has a total relief of about 260 m, as compared to the 800 m relief on the regional slope. An expanded view of the velocity field (fig. 10E) shows that flow rates approach a minimum where the two flow systems converge, near x = 265 km on the horizontal axis. Several sets of possible configurations (Garven, ms) show that this particular situation is one of the few hydrodynamic cases where mixing at the regional scale of fluids from different source areas could take place to form an ore deposit. Metal-bearing brines from one system could encounter H_2S-bearing fluids from the other, and mixing would occur under the influence of hydrodynamic dispersion where the flow systems converge.

CONTROLS ON SUBSURFACE TEMPERATURES

Quantitative modeling of heat transport has been carried out for a variety of purposes, including the study of geothermal reservoirs, heat storage in aquifers, radioactive-waste disposal, and hydrothermal circulation in the Earth's crust. The effect of regional groundwater flow on subsurface temperature patterns has also received study from a number of hydrologists. Stallman (1963) and Bredehoeft and Papadopoulos (1965) showed how groundwater flow rates can be estimated from observed temperature data. The influence of groundwater flow systems on heat flow in an idealized cross section was investigated mathematically by Domenico and Palciauskas (1973) who solved the heat-flow equation analytically. Parsons (1970) looked at a similar problem using finite-difference models. Both studies quantitatively demonstrated that convective heat transport results in a decrease in geothermal gradients in areas of groundwater recharge and an increase in geothermal gradients in areas of groundwater discharge. Betcher (ms) performed a sensitivity analysis of the parameters affecting heat flow in a hypothetical 10 km-long groundwater basin through the use of a finite-element model. Smith and Chapman (1983) also used a numerical approach to help explain how groundwater flow affects subsurface temperature profiles in hypothetical groundwater basins, as an aid in the interpretation of field data from heat-flow studies.

The purpose of the analysis presented here is to assess some of the important controlling factors of regional heat transport, especially in regard to their role in stratabound ore formation. Unlike previous studies, these numerical solutions provide for complete coupling with the fluid-flow equation in the simulation of temperature- and salinity-dependent fluid flow with thermal dispersion.

Simulations have been carried out to illustrate the effect of the fluid-flow regime, the boundary conditions, the thermal properties of porous media, and the basin geometry and water-table configuration on the temperature distribution in large basins. With the sensitivity analysis, various conditions are found that explain and support the temperature range of ore formation in sedimentary basins, as indicated by fluid-inclusion data of carbonate-hosted lead-zinc deposits. Quantitative insight is also provided on the role of groundwater flow in sustaining warm temperatures at shallow depths and near the edge of sedimentary basins — a problem that has been difficult to explain in the past when genetic models other than regional gravity-driven flow systems have been called upon.

To begin the analysis, let us consider the hydraulic effects on the temperature pattern in the two-layer basin that we have been studying thus far. For example, figure 5A displays the typical temperature pattern for the case of a basin with a linear water-table slope. It assumes that a constant geothermal heat flux of 60 mW/m^2 occurs along the entire length of the basement boundary. This heat flow value is representative of continental platform areas. The two lateral boundaries are assumed to be insulated barriers across which there is no heat transport. The water-table surface is an isothermal boundary where the temperature is assigned a value of 20°C to represent the mean air temperature. The lower layer is a dolomite aquifer with a horizontal hydraulic conductivity of 100 m/yr, a vertical hydraulic conductivity of 1 m/yr, a porosity of 0.15, and a thermal conductivity of 3.0 W/m°C. A constant value of 0.63 W/m°C is assumed for the thermal conductivity of the fluid throughout the basin. The upper layer is a shale aquitard with a horizontal hydraulic conductivity of 10 m/yr, a vertical hydraulic conductivity of 0.1 m/yr, a porosity of 0.10, and a thermal conductivity of 2.0 W/m°C. Specific heat capacities of 1005 J/kg°C for the rocks and 4187 J/kg°C for the fluid are assumed to remain constant.

Notice in figure 5A that the isotherms are not perfectly horizontal nor evenly spaced. The depression of the contours in the upstream end of the basin is caused by recharging fluid flow convecting heat down into the basal aquifer. Upward flow in the downstream end of the basin causes the warping of isotherms and the elevation of temperatures above that expected by thermal conduction alone. However, conduction still exerts a strong control on the temperature field, in spite of the groundwater flow system. This is evident in the near-horizontal character of the isotherms and in the spacing influence on the isotherms due to variations in thermal conductivity between layers.

The point to be emphasized here is that heat-flow patterns in sedimentary basins are the result of the boundary conditions and two important transport processes: conduction and convection. It is also important that temperature and salinity effects on water properties be included in the numerical modeling of heat transport, so as to account properly for their influence on convection.

Thermal conductivity.—In the absence of convection, temperature gradients are solely controlled by the boundary conditions on the thermal regime and by the thermal conductivity of the porous media. Table 4 gives the range of thermal conductivities for several types of geologic materials. These have been compiled from the listings of Clark (1966), Kappelmeyer and Haenel (1974), and Sass and others (1981). As shown in part 1, the effective thermal conductivity of the porous medium is a function of the fluid thermal conductivity, the rock thermal conductivity, and the porosity. Temperature also affects the thermal conductivity of rocks and water, but the influence is small for temperatures below 150°C. Porosity is set equal to a constant in the simulations given below, and only the thermal conductivity of the rock is varied.

Figure 11 shows the results of six simulations in which the thermal conductivity of the stratigraphic section is varied between 1.0 and 6.0

W/m°C. The basin is homogeneous with respect to the thermal properties, and a constant geothermal heat flux of 60 mW/m² occurs on the basement boundary. The surface temperature on the water table is a constant 20°C. The hydraulic properties of the two-layer basin are the same as those mentioned above. Temperatures in the downstream end of the basin appear to meet ore-genesis requirements of $T > 50°C$ for thermal conductivity (κ) values less than 3.0 W/m°C. This is a realistic upper limit to the average range of thermal conductivity for sedimentary-type lithologies (table 3). At the low end of the range, $\kappa = 1.0$ W/m°C, thermal gradients are much greater in the basin, and subsurface temperatures easily exceed 80°C in the downstream end of the basal aquifer. It appears that thick sequences of shale or limestone are conducive to maintaining ore-forming conditions of warm temperatures at relatively shallow depths. Simulations of heterogeneous thermal conductivity fields given in Garven (ms) show that for layered cases the temperatures in a basin are higher if less thermally conductive strata overlie more conductive strata.

Hydraulic conductivity.—Intuitively it makes sense that the process of heat convection will become stronger in a basin as fluid-flow rates increase. Conversely, the effect of thermal conduction dominates the thermal regime if flow rates are small. It was shown earlier that greater flow rates can be obtained either by increasing the hydraulic conductivity or by increasing the slope on the water-table surface. Coupling fluid flow with a temperature-dependent viscosity also provides a means for higher flow rates at depth in a sedimentary basin.

TABLE 4

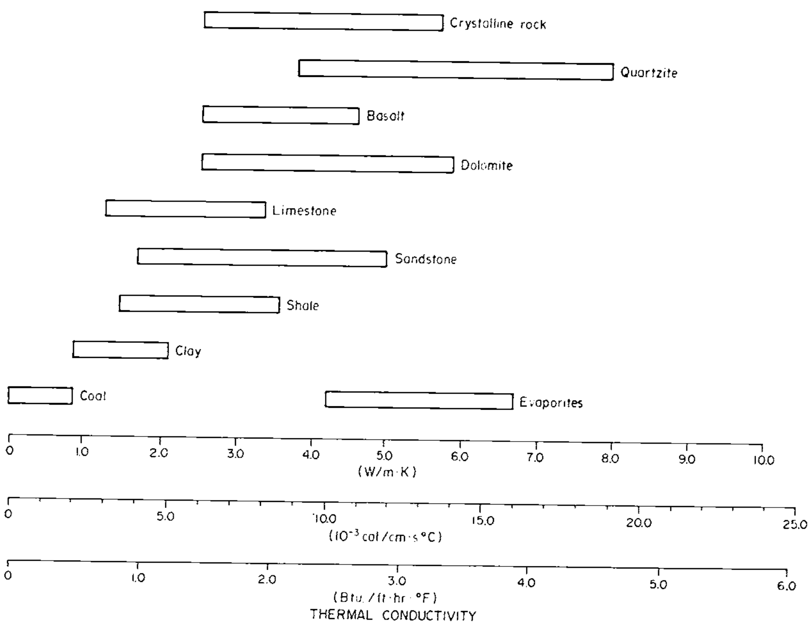

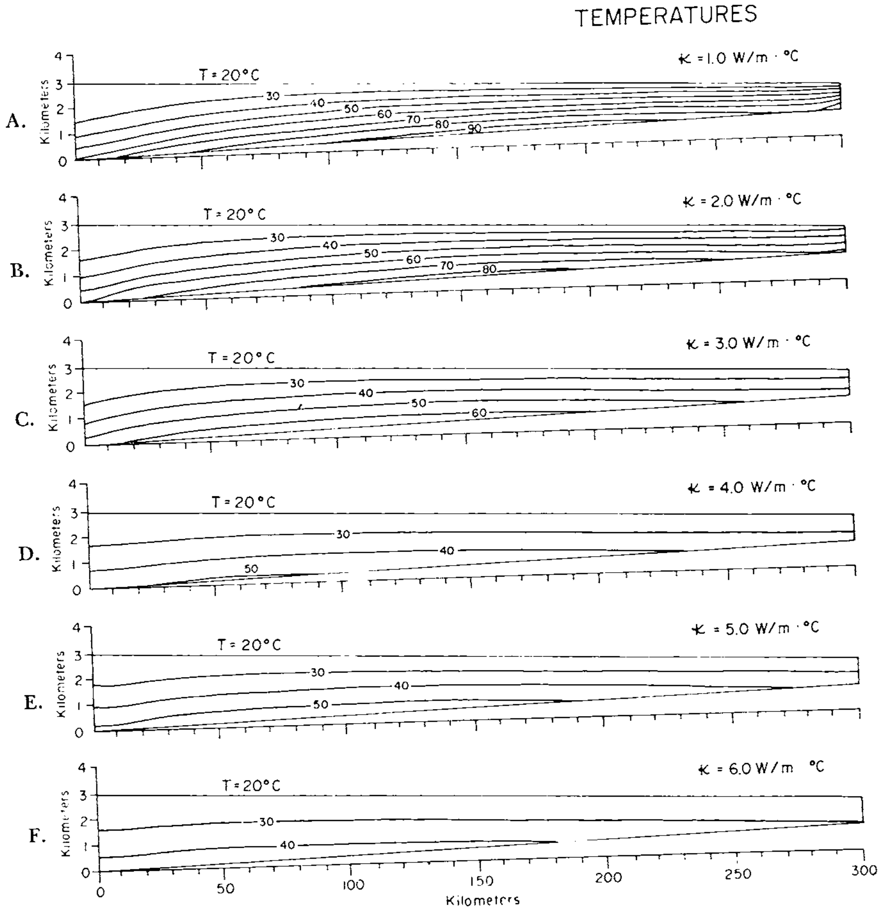

Fig. 11. Temperature patterns in thermally homogeneous basin for various values of thermal conductivity.

Figure 12 shows the quantitative results of some numerical experiments that were run to study the effect of hydraulic conductivity on heat flow. To isolate the effects, the thermal conductivities of the two hydrostratigraphic units are set equal to 3.0 W/m°C, and the thermal dispersivities are set equal to zero. Four separate results are shown in figure 12 for the basal unit horizontal hydraulic conductivity K_1 equal to: (A) 10^{-11} m/yr, (B) 10 m/yr, (C) 100 m/yr, and (D) 500 m/yr. The hydraulic conductivity in the upper unit, K_2, is appropriately adjusted in each case to maintain the permeability contrast of 10:1 between layers. An anisotropy ratio of 100:1 for hydraulic conductivity in both layers is also held constant. Figure 12A is a case of almost pure conduction; figure 12D is a case of almost pure convection. The nature of the convective effect is summarized in figure 13. It is a plot of the average temperature in the basal layer as a function of distance along the wedge-shaped basin for the four simulations. Notice how the "hinge-point" at which the convective profile intersects the pure conduction profile is shifted downstream from point A to point B as the model hydraulic conductivity is increased. Under the given hydraulic and thermal properties of this two-layer basin model, gravity-driven flow systems can begin to affect temperatures in the basin where the horizontal hydraulic conductivity of the basal layer exceeds 10 m/yr. If the hydraulic conductivity is set at an unrealistically high value, simulated basin temperatures may become nearly isothermal.

It is clear that convective transport of heat can help explain the association of "anomalously high" temperatures at shallow depths with the association of many stratabound ores near a basin margin. In a gravity-driven flow system, not only is the presence of an aquifer essential in focusing flow to an ore-forming site, but it also provides a means for elevating temperatures at the thin edge of a basin.

Thermal dispersivity.—The coefficients of thermal dispersivity, ϵ_L and ϵ_T, are the least known parameters in the heat-transport equation. Results from a detailed assessment of thermal dispersivity (Garven, ms) in the basin model of figure 5 showed that varying the dispersivity had little visible effect on regional steady-state temperature patterns. Theoretical discussions of the effects of thermal dispersion at a local scale can be found in Rubin (1974), Weber (1975), and Tyvand (1977).

Geothermal heat flow.—The simulations presented thus far have considered a prescribed basal heat flux of 60 mW/m^2 as being representative of continental platforms. Field measurements of present-day

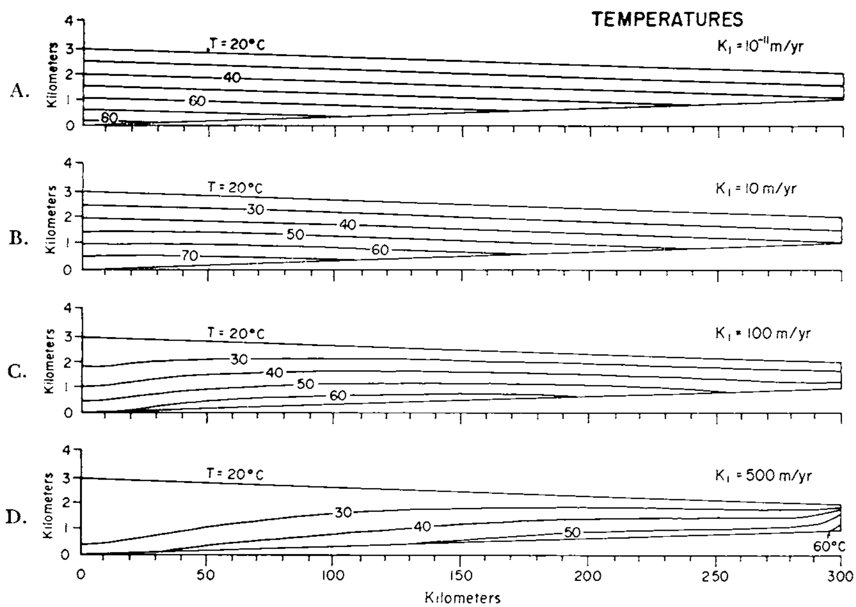

Fig. 12. Temperature patterns showing the effects of convection for various values of hydraulic conductivity of a basal aquifer unit.

regional heat flow may vary from about 40 mW/m² in stable granitic shields to over 120 mW/m² in tectonically active regions (Sass and others, 1981). Heat flow can exceed 200 mW/m² in some geothermal environments. Intermediate heat fluxes between J = 50 to 100 mW/m² are likely to be the most realistic range of values in sedimentary basins.

Garven (ms) has carried out a number of simulations for a case similar to that of figure 5 but with varying values of the basal heat flux J. Figure 14 summarizes the results by giving a set of temperature profiles with depth on a line that passes through point A (fig. 5C). Doubling the heat flux from 50 to 100 mW/m² causes the basal temperature to increase from 58° to 99°C.

These results do not account for the temperature values around 150°C, which is estimated for some lead-zinc ores in the Mississippi Valley district. Other factors, such as higher geothermal fluxes, lower thermal conductivities, or thicker basins, must play a role in producing high-temperature environments for stratabound ore formation. However, heat-flow values of 60 to 80 mW/m² (Jessop and Lewis, 1978) appear to be adequate for the size and thickness of the basin modeled here, to satisfy the thermal conditions estimated for lower temperature ranges of lead-zinc ore deposition.

Climate and heat flow.—Climatic conditions are included in the heat-flow model through the specification of the surface temperature, T_0, on the water-table boundary. For simplicity, the same mean annual sur-

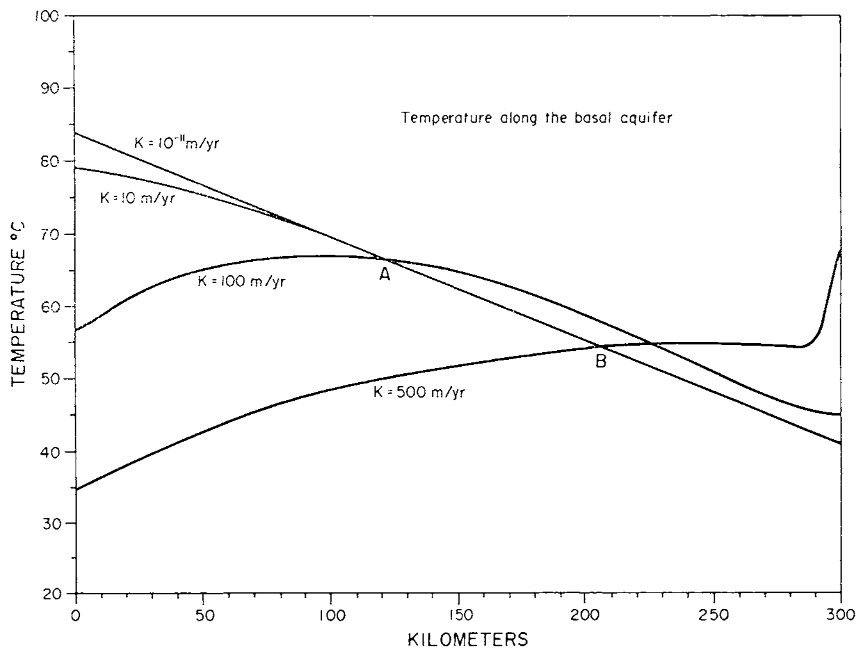

Fig. 13. Effect of hydraulic conductivity on the temperature along a basal aquifer.

face temperature is prescribed over the entire length of the basin. Changing the surface-temperature condition by 10°C causes a general numerical change in each isotherm by about 10°C, although the effect is not exactly linear (Garven, ms). If we are willing to accept a heat flux $J = 80$ mW/m² as a reasonable upper limit (fig. 14), then the maximum temperature in the basin model will range between 85° and 105°C for the surface-temperature range of 10° and 30°C. Climatic conditions were apparently favorable for this temperature range for much of the Paleozoic and Mesozoic eras on the North American continent.

Basin geometry.—The effect of basin size on subsurface temperature is shown in figure 15. The length-to-depth ratio of each basin is 100:1, and the material properties of the two-layer basin are the same as before. A basal geothermal flux of 60 mW/m² and a surface temperature of 20°C are assumed constants. Fluid velocities in the bottom, high-permeability layer average around 2.5 m/yr for the basin models where the length is less than 300 km, but velocities reach values as high as 7.2 m/yr in the 600-km long basin (fig. 15D). Temperatures easily exceed 100°C in the basal part of the gravity-driven flow system at the downstream end of this large basin. Perhaps it is this scale of flow system, with fluid circulation to depths of 6 km in the thick basins, that is responsible for the formation of lead-zinc ores at the higher end of their temperature range (100°-150°C), as in the Mississippi Valley district. A high geothermal flux such as 80 mW/m² and surface temperature of 30°C could raise temperatures well above 150°C in the discharge end of the basin. There is no need,

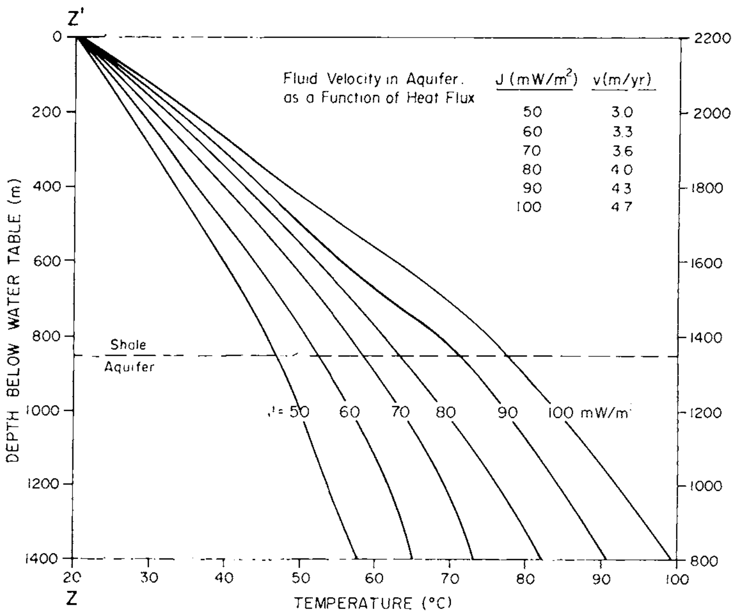

Fig. 14. Temperature profile in the downstream end of the two-layer basin as a function of the geothermal flux.

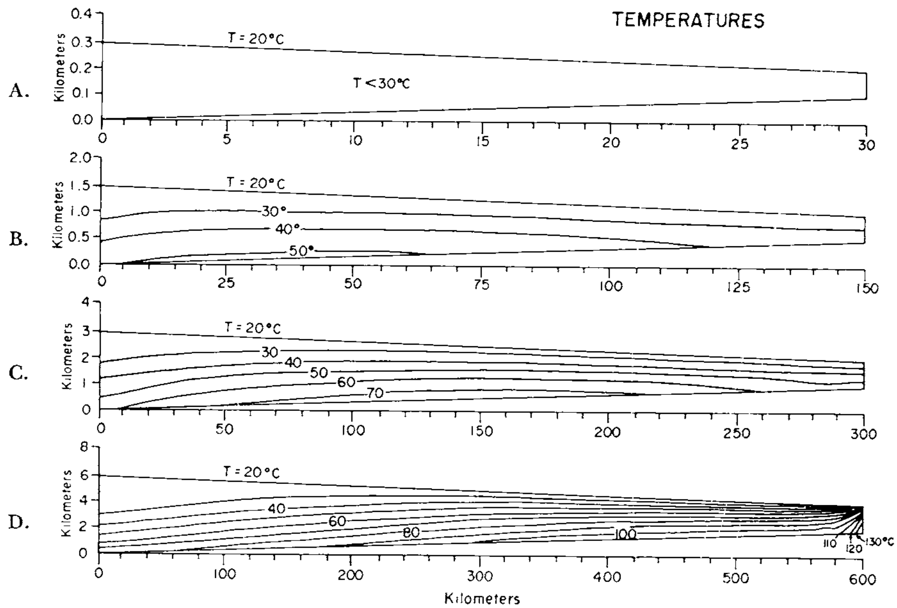

Fig. 15. Control of basin size and thickness on subsurface temperatures.

therefore, to invoke unknown heat sources within the basement to explain the warm temperatures associated with some forms of stratabound ore genesis.

Basement structure like that shown in figure 8 affects the thermal regime in a sedimentary basin, mainly through its influence on the hydrodynamics. Figure 16 shows the basal aquifer temperature for the few cases discussed with respect to figure 9. Notice how effective a basement arch is at reducing the convective transport of heat from the thick part of the basin to the thin basin margin. This feature bears out the importance of long continuous flow systems in the development of adequate temperatures at shallow depths and near the edge of a basin. On the other hand, basement arches between adjoining sedimentary basins may themselves serve to form suitable thermal and hydraulic conditions for ore genesis. Remember, the absolute temperatures in figure 16 could be 10° to 30°C higher, under warmer climatic conditions, lower thermal conductivities, or higher values of geothermal heat flux.

Water-table configuration.—The configuration of the water-table affects subsurface temperatures in two ways. First, it forms a thermal boundary of constant temperature, which thereby exerts control on the shape of the isotherms and ultimately thermal gradients. Second, the strong control of the water-table configuration on the groundwater flow systems means that heat transport will in turn be affected through convection processes. The influence of both factors are illustrated in the simulations given in figure 17 for various water-table configurations of the sloping-bottom, two-layer basin. The geothermal heat flux on the bottom boundary is 60 mW/m^2.

The presence of a slight break in topographic slope in figure 17A appears to modify the temperature pattern only slightly. Introducing a water-table ridge at the end of the basin has a greater effect on bending the isotherms near the base of the rise (fig. 17B). Upward and downward heat transport effects are associated with locally-elevated highs in any part of a basin. Major topographic lows serve to focus groundwater discharge, which in turn creates anomalously high temperatures at relatively shallow depths (fig. 17D). The last temperature pattern in figure 17 shows how a complicated water-table configuration is reflected in irregular perturbations on the isotherms.

It is apparent from these simulations that major topographic features within a basin serve to develop zones of downward heat convection in recharge areas and upward heat convection in discharge areas. As in the case of fluid flow, the heat-transport system can be weakly or strongly modified, depending on the topographic relief, the basin size and structure, and the material properties of the hydrostratigraphic units. The genetic association between anomalously warm temperatures and stratabound ores is clearly linked to groundwater discharge features at a regional scale.

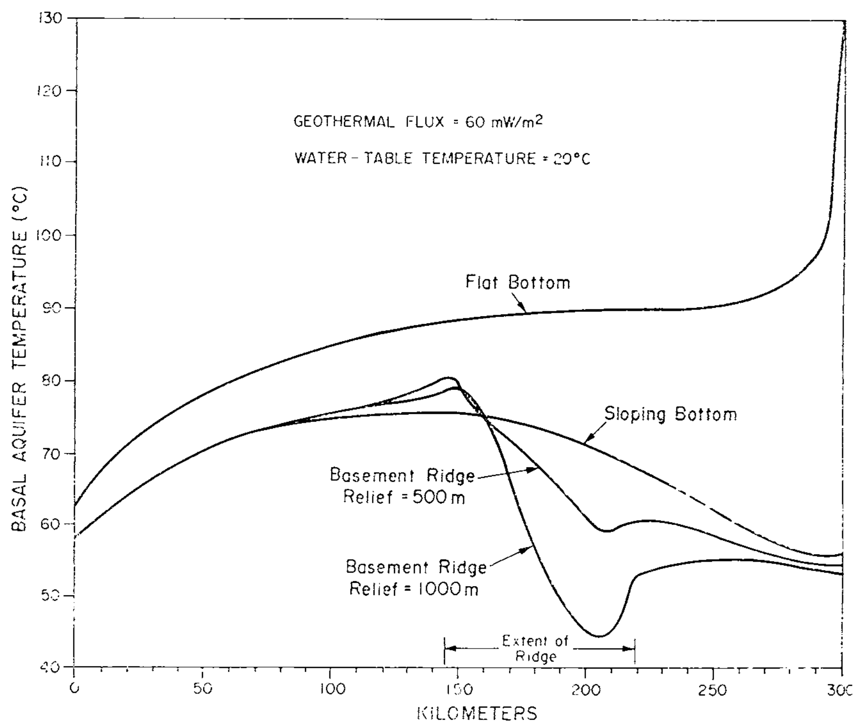

Fig. 16. Temperature along the basal aquifer as a function of basement structure.

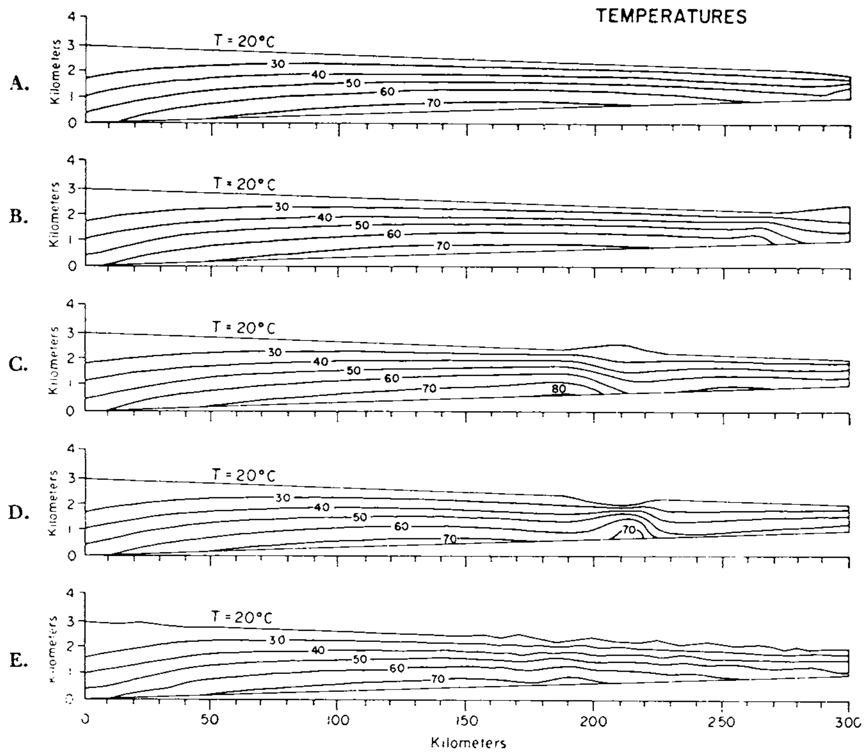

Fig. 17. Control of water-table configuration on subsurface temperatures.

CONTROLS ON MASS TRANSPORT

As a metal-bearing brine flows through a basin, the concentration of its aqueous components vary along the flow path. These variations can be caused by a number of geochemical and hydraulic processes. In the absence of fluid mixing and geochemical reactions, an ideal tracer solute will travel at a rate equal to the average linear velocity of the groundwater, and its concentration will remain unchanged. However, even in the case of a conservative solute passing through a nonreactive porous medium, the processes of mechanical mixing and molecular diffusion result in a spreading of the solute, both longitudinal and transverse to the flow direction, which results in a decrease in the original concentration of the aqueous component. This spreading process is called hydrodynamic dispersion. It is a physical phenomenon that exists in nature and therefore must be included in an analysis of transport. The formation of an ore deposit requires that the fluid-flow system leach background amounts of ore-forming constituents from over wide areas and focus these components in a specific part of the basin. This focusing of mass is represented by the increase in flow rates, as shown in several of the preceding simulations. In a mature sedimentary basin, gravity-driven flow systems provide a natural mechanism for focusing of flow near the basin margin through the influence of the hydrostratigraphy and water-table configuration. In spite of the favorable hydrodynamic conditions, the process of dispersion may lead to unfavorable conditions for the formation of ore deposits. It is the relative balance between the hydraulic focusing of flow lines in discharge areas and the spreading effects of dispersion that controls whether sufficient masses of ore-forming species arrive at potential ore-forming sites.

The general subject of solute transport in porous media has received a tremendous amount of theoretical and applied research. Hydrogeologic studies, such as those by Pickens and Lennox (1976), Schwartz (1977), and others, have sought to demonstrate the importance of various factors on dispersion in groundwater flow systems. The simulations given below review some of the important factors affecting mass transport in large sedimentary basins, with specific reference to ore genesis. Many of the effects, which are directly dependent on the advection patterns of mass, are self-evident from the fluid-flow patterns already presented. The fluid-flow velocities from these simulations also allow the determination of travel times, mass-flux rates, and the time required to deposit a large ore body for a given rate of precipitation at an ore-forming site.

In this section, the emphasis is placed on the quantitative aspects of mass transport in basins. Attention is focused on the problem of understanding how the concentration of an ore-forming component reaching a depositional site depends on the original concentration released in the source bed, the length of the flow path, the rate of flow, and the degree of dilution caused by dispersion along the flow path. This type of information is needed when making realistic estimates of the metal concentrations in a brine passing through an ore-forming site. The transport simulations performed here do not simulate the geochemical process of releasing metals from source bed to the fluid or the reactions along fluid pathlines. When reference is made to the solute, it is usually meant to describe a metal species, but the modeling results are equally valid for any aqueous species, including sulfide, because of the theoretical assumptions made in part 1. Three controlling factors are now examined below: the effect of dispersion coefficients, the effect of hydraulic parameters, and the effect of geology.

Dispersivity.—As shown in part 1 of this study the dispersion coefficient consists of two components, a term representing mechanical dispersion and a term representing the effective molecular diffusivity. The mechanical dispersion term is formulated as the product of the medium dispersivity and fluid velocity. This component is zero only when there is no fluid motion in a porous medium.

Diffusion coefficients for aqueous species commonly range from 10^{-9} to 10^{-12}m^2/s in porous media (Freeze and Cherry, 1979). Compared to mechanical dispersion, molecular diffusion is several orders of magnitude smaller, unless fluid-flow rates are very low. A constant diffusivity of

$10^{-12} m^2/s$ is used in this study, but in all cases its effect as a viable transport mechanism in ore genesis is negligible.

Dispersivity values reflect the nature and scale of heterogeneities in the flow system. Table 5 summarizes the range of dispersivities that have been suggested for various geologic materials (after Anderson, 1979). Representative values for the basin being modeled in this study are thought to range between 10 and 500 m for the longitudinal dispersivity α_L. The transverse dispersivity α_T is expected to be lower in value by a factor of 1 to 100.

To test the sensivity of the two-layer basin model to the dispersivity parameters, a series of simulations were run where these coefficients are varied. All other parameters were kept constant. The basal layer is assumed to have a horizontal hydraulic conductivity of 200 m/yr and a constant porosity of 0.15. The overlying layer has a horizontal hydraulic conductivity of 10 m/yr and a porosity of 0.10. An anisotropy ratio of horizontal to vertical hydraulic conductivity of 100:1 is once again assumed for both hydrostratigraphic units.

Figure 18 summarizes the results from one set of mass-transport simulations. In this case, the dispersivity parameters are constant throughout the basin, and $\alpha_L = \alpha_T$ in both layers. The fluid-flow system (fig. 18A) remains the same in all the simulations. Mass is instantaneously released at t = 0 yr from source beds at a point located in the recharge end of the basin (fig. 18B). Figure 18 shows the position and shape of the concentration plumes at two selected periods in time: t = 20,000 yr and t = 40,000 yr. Four separate simulation results are given, with dispersivity values of 1, 5, 10, and 50 m respectively. Only relative concentration contours of 5, 10, and 15 percent C/C_0 have been plotted for comparison purposes.

If there is no dispersion in a flow system a dissolved metal species will move along a flow path as plug-type flow, and there will be no change

TABLE 5

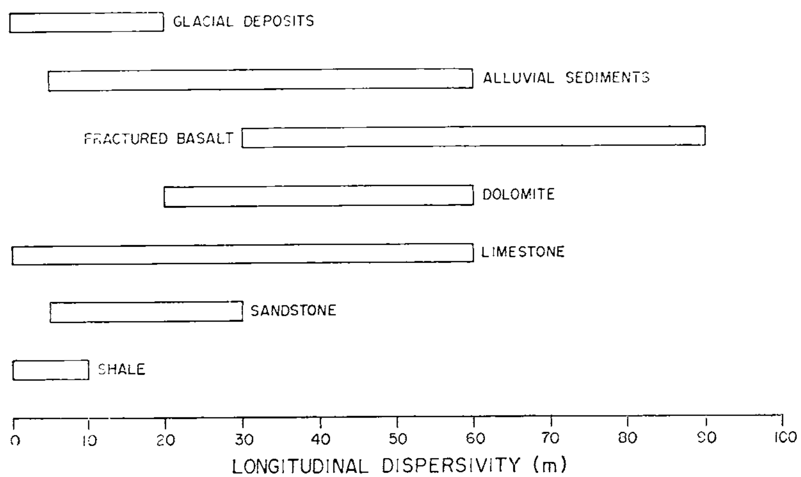

in concentration between the points of entrance (source beds) and exit (ore-forming site). In figure 18B, the maximum concentration of the pulse averages nearly 35 percent C/C_0 at $t = 40{,}000$ yr for $\alpha_L = \alpha_T = 1$ m. Increasing the dispersivity causes further dilution of the solute along the flow path. The maximum value of C/C_0 decreases to about 15, 10, and 5 percent for $\alpha = 5$, 10, and 50 m. Realistic estimates of the concentration of metal in brines reaching an ore-forming site near the discharge end of a basin clearly depend on taking into account the dilution effect of dispersion. The implications of this factor in light of the metal concentrations imposed by solubility constraints is discussed later.

A more accurate field situation is simulated when the individual geologic units are assigned separate dispersivity values with the longitudinal component larger than the transverse component. A set of simulations presented by Garven (ms) demonstrates the influence of longitudinal dispersivity on transport patterns in such systems.

Hydraulic conductivity.—Consider the simple, two-layer basin with a sloping basement and linear water-table slope. Groundwater flow is directed downward across the shale beds of the upper unit in the elevated end of the basin, it flows laterally through the basal aquifer unit in the

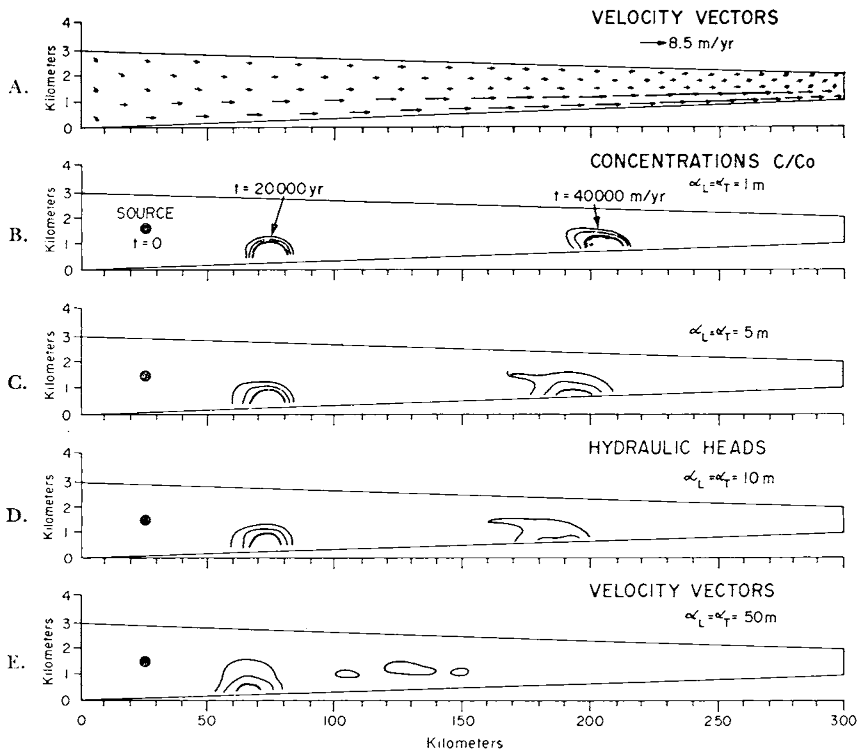

Fig. 18. Effect of isotropic and homogeneous dispersivity on the mass-transport patterns in a two-layer basin.

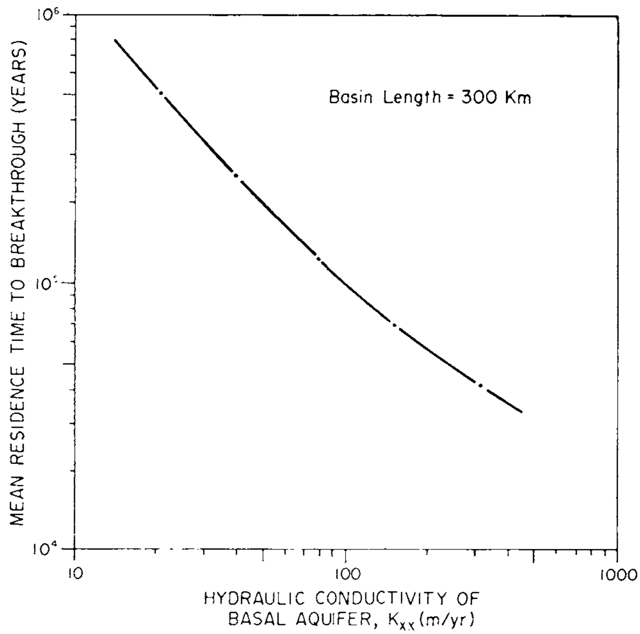

Fig. 19. Relationship between the average basin-residence time for a metal-bearing pulse and the hydraulic conductivity of the basal aquifer in a two-layer basin model.

mid-section of the basin, and it is forced upward back across the shale beds near the basin margin. Transport of mass in the system conforms to the fluid-flow pattern and the effects of dispersion. Advective transport by the flow system controls the path of transport, and dispersive transport causes the solute mass to spread as it moves through the flow system. Figures 2 to 10 have shown how advection patterns are controlled by the hydrostratigraphy, the basin geometry, and the water-table configuration. The flow pattern remains nearly the same for any fixed contrast in the hydraulic conductivities between the layers, but the fluid velocity depends on the actual magnitude of the hydraulic conductivities and the basin geometry. As mentioned earlier, these factors, therefore, will control the actual rates of mass transport through a basin and also the amount of dispersive transport because of its dependence on the fluid velocity.

Keeping other basin parameters constant while varying the hydraulic conductivity causes transport rates to increase or decrease according to the change in the hydraulic conductivity, as shown in figure 19. The time it takes for the center of mass of a metal-bearing pulse (fig. 18) to break through to the water-table surface is plotted as a function of the horizontal hydraulic conductivity of the basal unit in a two-layer basin. The curve is drawn according to the results of several simulations, based on estimates of a realistic range of hydraulic conductivity. A permeability contrast of 20:1 was maintained between the two layers, as was the anisotropy ratio of 100:1 for the hydraulic conductivity. The dispersivity was assumed to be a constant 1 m in the upper shale beds, but in the lower aquifer unit the dispersivities were assumed to be $\alpha_L = 10$ m and $\alpha_T = 1$ m. For the case where $K_{xx} = 80$ m/yr, the concentration pulse takes about 110,000 yr to pass through the section.

It should be reiterated that the mass transport process is being represented as a transient event of metals entering the flow system at a given point (fig. 18B) and being transported through the basin. We are modeling this process numerically as a pulse of tracer particles spreading through the section. This is *not* to imply that ore formation is the result of a single pulse of metal-bearing brine or even a set of discrete pulses. The representation used here is simply a mathematical approach for simulating the concentration levels and transport paths as brines continuously flow through the basin. It is the *continuous* leaching and transport over geologic time by gravity-driven groundwater flow that eventually results in the formation of a sizeable ore deposit, provided adequate flow rates can be maintained and the geochemical conditions are suitable for ore precipitation.

Varying the hydraulic conductivity should also modify the amount of dispersion in a flow system because of its dependence on fluid velocities. Higher permeabilities allow greater flow rates which in turn lead to greater amounts of dispersion and larger rates of advection (fig. 19). Overall, the mass transport pattern remains nearly the same, at least for the case where the hydraulic conductivity is only varied over the order-of-magnitude range shown in figure 19. This sensitivity result is illustrated in figure 20, in which the maximum pulse concentration in the basal aquifer is plotted as a function of lateral distance along the basin, for several simulations. The solid curve is drawn with some artistic license to indicate the general trend of the solute concentration in a schematic form. About 20 percent of the original, source-bed concentration level C_0

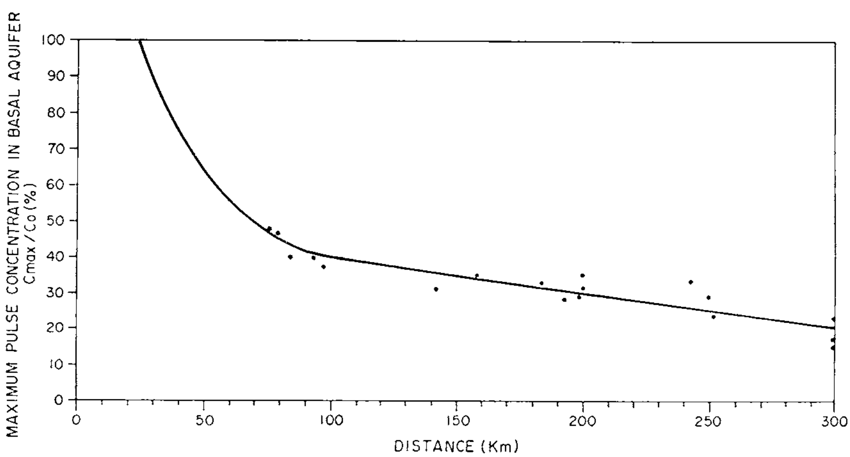

Fig. 20. Maximum solute concentration in the basal aquifer as a function of transport distance.

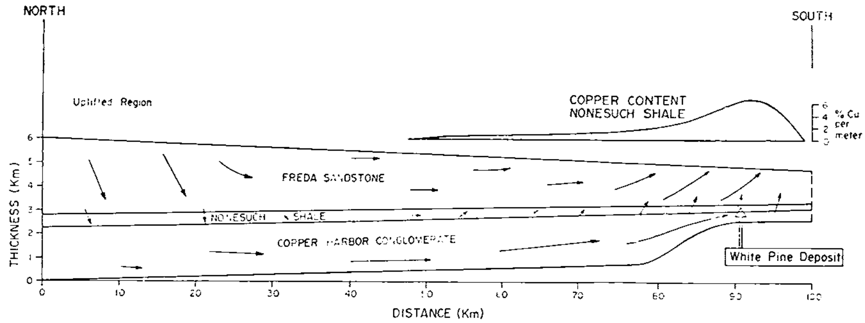

Fig. 21. Conceptual model of fluid flow in the Lake Superior basin at the time of formation of the White Pine copper deposit and copper content of the Nonesuch Shale (geology modified after White, 1971).

is present in the basinal brine as it passes through the aquifer at the basin margin. Based on this result, if a metal concentration of 1 mg/kg H_2O is accepted as a minimum requirement for ore formation (Anderson, 1978), then a minimum source concentration of about 5 mg/kg H_2O is required in the upstream end of a 300-km basin flow system. Although this transport model is simplified because it does not explicitly account for the gain or loss of metal through reactions along the flow path, it does provide for a more realistic assessment of the role of fluid flow in ore formation than a simpler plug-flow calculation.

Geology.—Garven (ms) reports on over twenty detailed transport simulations conducted on specialized geologic configurations containing various types of stratigraphic and structural features. Each of these models displays a unique fluid-flow pattern, subsurface temperature distribution, and concentration pattern that arise from the specific geologic setting. Whatever the nature of the stratigraphy, however, aquifers (or beds with relatively higher hydraulic conductivity) serve to focus flow such that basinal fluids flow along the path of least resistance. The existence of discontinuous aquifers in a basin generally results in an upward movement of flow near the edge of the aquifer, whether or not the pinchout is caused by a facies change, faulting basement structures, or unconformities. Localized high-permeability zones such as carbonate reef structures do not create major alterations in the regional transport patterns.

As an example of the type of field setting where the concepts of this study appear to have significance, consider figure 21, which is a schematic cross section through the Lake Superior basin at the time of formation of the White Pine copper deposit. The geology of the right-half of the section is from the study by White (1971). The flow arrows depict a conceptualized fluid-flow pattern based on an interpretation of the gravity-driven groundwater model proposed by White (1971) to explain copper mineralization in the Nonesuch Shale at White Pine, Mich. Copper-bearing fluids flowed through the basal conglomerate aquifer toward the edge of the Lake Superior basin and were eventually forced upward and through the Nonesuch Shale. Copper precipitation was caused by replacement of pre-existing iron-sulfide minerals in the shale beds (Brown, 1971). The presence of a widespread reactant (that is, pyrite) allowed the development of a well-defined mineralization pattern, with maximum ore grades, where upward transport rates were probably highest (Garven, ms). The localization of the ore deposit at White Pine may be due to the presence of the basement arch, which served to focus upward discharge as in figure 8.

GEOCHEMICAL MODELS OF TRANSPORT AND PRECIPITATION

Fundamental to any hydrodynamic model of ore genesis in sedimentary environments is the concept of an original source bed from which metal species and/or sulfur can be expelled into the aqueous phase and transported to an ore-forming site. The exact process by which metals are released from source rocks is not always clear. Anderson and Macqueen (1982) suggest that the leaching of metals may take place through desorption phenomena, recrystallization processes, and thermal alteration of metal-organic complexes. Whatever the mechanism, field observations and experimental studies confirm that chloride-rich brines are very effective at leaching background amounts of metals from various rock types (Ellis, 1968; Bischoff, Radtke, and Rosenbauer, 1981; and others). Although the relatively higher metal contents of shale make it a favored source-bed lithology (Hitchon, 1981), granite, volcanic tuffs, carbonates, evaporites, feldspathic sandstone, and redbed cements have also been considered as suitable source beds by various authors.

The presence of chloride-rich brines in ore-forming environments is well-documented for stratabound deposits by fluid inclusion data which have proven the composition of the ore-forming fluids as being dominated by sodium–calcium–chloride brines with salinities of 10 to 30 percent NaCl equivalent (Roedder, 1976). How brines originate, even in present-day flow systems, is more problematic. In most cases, the formation of brines can be qualitatively attributed to the dissolution of evaporitic lithologies (or other forms of water-rock interaction) and membrane filtration processes. Both processes are probably aided by the slowly-moving nature of the groundwater and warm temperatures at depth. Bredehoeft and others (1963) presented a mathematical model for membrane filtration that predicts salinity profiles that compare well with present-day observations. Other types of processes may be equally important. It is because of these uncertainties that the simulations presented earlier assumed an arbitrary, linear salinity gradient. The work by Billings, Kesler, and Jackson (1969), Carpenter, Trout, and Pickett (1974), and Hitchon (1977) support the hypothesis that present-day basinal brines represent modern geochemical analogs of past ore-forming fluids.

The geochemistry of metal transport and sulfide precipitation has received a large amount of theoretical and experimental research. With specific reference to carbonate-hosted lead–zinc deposits, recent studies that review the state-of-the-art of geochemical models of this ore association include Anderson (1978), Giordano and Barnes (1981), Sverjensky (1981, 1984), Anderson and Macqueen (1982), and Barrett and Anderson (1982). The formation of complex ions in solution is now known to be the primary mechanism for the geochemical transport of metal species in ore-depositing flow systems (Skinner, 1979). Complexing substantially increases the solubilities of metals, and it provides a means for the long-distance transport of metals in fluid-flow systems. Both chloride complexes and sulfide complexes have been called upon to explain metal transport in ore genesis (Helgeson, 1964; Barnes and Czamanske, 1967). Chloride complexes form in the presence of high concentrations of chloride ion and can transport large amounts of lead and zinc in solution, provided the sulfide concentrations ($H_2S(aq)$, HS^-) are low. Modest amounts of metal and sulfide may be transported together in equilibrium, but the brine must be acidic in character (Anderson, 1973). Bisulfide complexes form in the presence of high concentrations of aqueous sulfide and can transport small amounts of base metals under alkaline conditions, thereby overcoming the problem of transporting acidic solutions through carbonate strata.

The relative importance of these two complexes is still debated. In both cases, one of the ore-forming components must be at a low concentration in order to transport large quantities of the other component over long distances. Of course, one can completely avoid the constraints imposed by equilibrium transport of metal and sulfur by invoking a third model where two separate fluids, each carrying one of the ore-forming components, mix at a common point of discharge.

Table 6 contains a summary of three basic geochemical models proposed for ore formation in sedimentary basins. The possible mechanisms of ore precipitation are also listed for each model. Detailed discussions on these mechanisms are given elsewhere in the literature (Anderson, 1973,

TABLE 6

Transport model	Reasons for deposition
I. Metals transported in low-sulfur fluid	A. Mixing with H_2S-bearing solutions B. Replacement of iron sulfides C. Thermal degradation of organics
II. Metals transported in sulfate-bearing fluid	A. Sulfate reduction by bacterial destruction of organics to produce H_2S B. Sulfate reduction by non-bacterial destruction of organics to produce elemental sulfur C. Sulfate reduction internally due to methane D. Sulfate reduction externally on encountering petroleum E. Sulfate reduction due to reaction with iron-bearing minerals
III. Metals and sulfide transported together in the same fluid	A. Reaction with host rock and rise in pH B. Temperature drop C. Decreased stability of chloride complexes due to mixing

1975; Giordano and Barnes, 1981; Sverjensky, 1981), and an explanatory overview can be found in Garven (ms). Only two of the geochemical models are evaluated in this study, using simulations provided by EQ3/EQ6. First to be considered are the type II models (table 6), which propose that the metals are transported in a sulfate-bearing brine and that ore precipitation occurs at sites where the sulfate is reduced locally to sulfide. Secondly, the type III geochemical conditions necessary for simultaneous transport of metal and sulfide in the same fluid are examined, and possible precipitation mechanisms tested. Carbonate-hosted lead–zinc deposition serves as the simulation example.

Mixing-type models that assume transport of metal in one fluid and sulfide in another are not explicitly assessed in this evaluation. We have already seen from the fluid-flow and mass-transport modeling that the transport of two immiscible fluids is highly unlikely in long-distance brine transport, because of the regionally continuous nature of flow systems in sedimentary basins and because of mixing between flow lines through dispersion. On the other hand, some hydrogeologic conditions are capable of supplying to mixing areas one or the other ore-forming components from different parts of a basin. This is accomplished through the development of local flow systems, which are superimposed on regional flow systems (fig. 10).

Metal-sulfate brine model.—Consider the model of a metal-bearing brine containing sulfate (SO_4^{2-}). Table 7 outlines the composition of a hypothetical 2.0 molal NaCl brine at a temperature of 75°C. The concentration values are chosen to be representative of a deep, basinal brine in equilibrium with carbonate strata through which it is flowing. They are based partly on the observed composition of present-day oil-field

TABLE 7

$T = 75°C$
$pH = 5.0$
$f_{O_2} = 10^{-50}$ $f_{CO_2} = 5$ bars
($Eh = +0.014$ volts)

Component	Concentration totals (moles/kg)	Concentration totals (mg/kg)
Na	1.46	30,030
K	5.0×10^{-2}	1,746
Ca*	2.4×10^{-1}	8,710
Mg**	9.2×10^{-3}	200
SiO_2(aq)	2.0×10^{-4}	5
Cl	2.0	63,330
SO_4	5.0×10^{-3}	145
H_2CO_3(app)†	4.2×10^{-2}	2,160
Fe	5.0×10^{-9}	2.5×10^{-4}
Zn††	1.0×10^{-4}	6.0
Pb	1.0×10^{-6}	0.2

* Calcite saturation.
** Dolomite saturation.
† $H_2CO_3(app) = CO_2(aq) + H_2CO_3(aq)$.
†† Total zinc content = $Zn^{++} + ZnCl^{+} + ZnCl_2 + ZnCl_3^{-} + ZnCl_4^{2-}$.

brines (White, 1968; Hitchon, Billings, and Klovan, 1971; Carpenter, Trout, and Pickett, 1974; Hitchon, 1977, 1981; Land and Prezbindowski, 1981); partly on fluid-inclusion analyses (Roedder, 1967; and subsequently many others); and partly on theoretical considerations (Anderson, 1973, 1975, 1977, 1978; Sverjensky, 1981; Helgeson, 1969; Kimbell, 1979; Barrett and Anderson, 1982). Garven (ms) reviews the contributions of these various authors and summarizes the geochemical constraints they suggest. In particular, Garven (ms) discusses the choice of pH, CO_2 partial pressure, Pb and Zn concentrations, sulfate-sulfide ratios, and total sulfur content. In addition, he discusses the solubilities of galena and sphalerite in brine and reviews their dependence on reduced sulfur concentration, salinity, and temperature.

Based on thermodynamic considerations, a wide variety of geochemical conditions will allow a metal-sulfate brine to carry sufficient lead or zinc to form a major ore deposit, provided some sort of sulfate-reduction process occurs (table 6). Three reaction-path simulations are now presented to demonstrate some of the possibilities.

The first numerical experiment to be considered involves the addition (titration) of $H_2S(g)$ to the model brine of table 7. It is assumed that sulfate in the fluid has been reduced to H_2S at the ore site. The actual reaction of sulfate reduction is not simulated, only that a source of H_2S is suddenly available. The amounts of lead and zinc chosen here are 10^{-6} *m* Pb and 10^{-4} *m* Zn (table 7). These numbers are not meant to simulate a metal ratio from any particular known ore environment but are simply assumed as reasonable concentrations based on known solubility data.

Figure 22 shows the results of one reaction-path simulation with EQ3/EQ6 where 10^{-3} *m* (34 mg/kg H_2O) of $H_2S(g)$ are dissolved into the metal-sulfate brine. The amounts of secondary minerals produced or destroyed and the composition of the aqueous phase are plotted as a function of the amount of the reactant $H_2S(g)$ dissolved. Only a selected set of the group of aqueous species are plotted in the speciation diagram. The 2.0 *m* NaCl brine is assumed to be initially in equilibrium with dolomite and limestone at a temperature of 75°C.

As H_2S dissolves, the aqueous sulfide species gradually become more concentrated. The solution is initially oversaturated with respect to dolomite because of the sudden change in the oxidation state. The result is the precipitation of dolomite (fig. 22) as the oxygen fugacity drops from 10^{-50} to 10^{-57}. With an adequate transfer of H_2S to the aqueous phase, hydrogen ion activity increases, and the availability of free sulfide and zinc leads to the oversaturation of the fluid with respect to sphalerite. This is marked by the precipitation of sphalerite and dissolution of dolomite near the point where the H_2S dissolved equals 10^{-7} *m*. Precipitation of sphalerite is also reflected in the change in concentrations of the free-metal species and zinc–chloride complexes. Galena is the next mineral phase to precipitate after sphalerite, and with the small amount of iron present in the system eventually pyrite is deposited. Most of the metal content of the fluid is exhausted by the stage at which 10^{-4} m H_2S have been dissolved, and the fluid is in equilibrium with the sulfide minerals. Approx 10^{-4} moles (10 mg) of sphalerite, 10^{-6} moles (0.3 mg) of galena, and 10^{-8} moles (0.001 mg) of pyrite are precipitated per kg of H_2O. These figures can be compared to the simulation example given in part 1 (fig. 8K), in which the brine is initially at a pH = 6.8, and the zinc concentration is an order of magnitude lower. Reacting this type of metal-sulfate

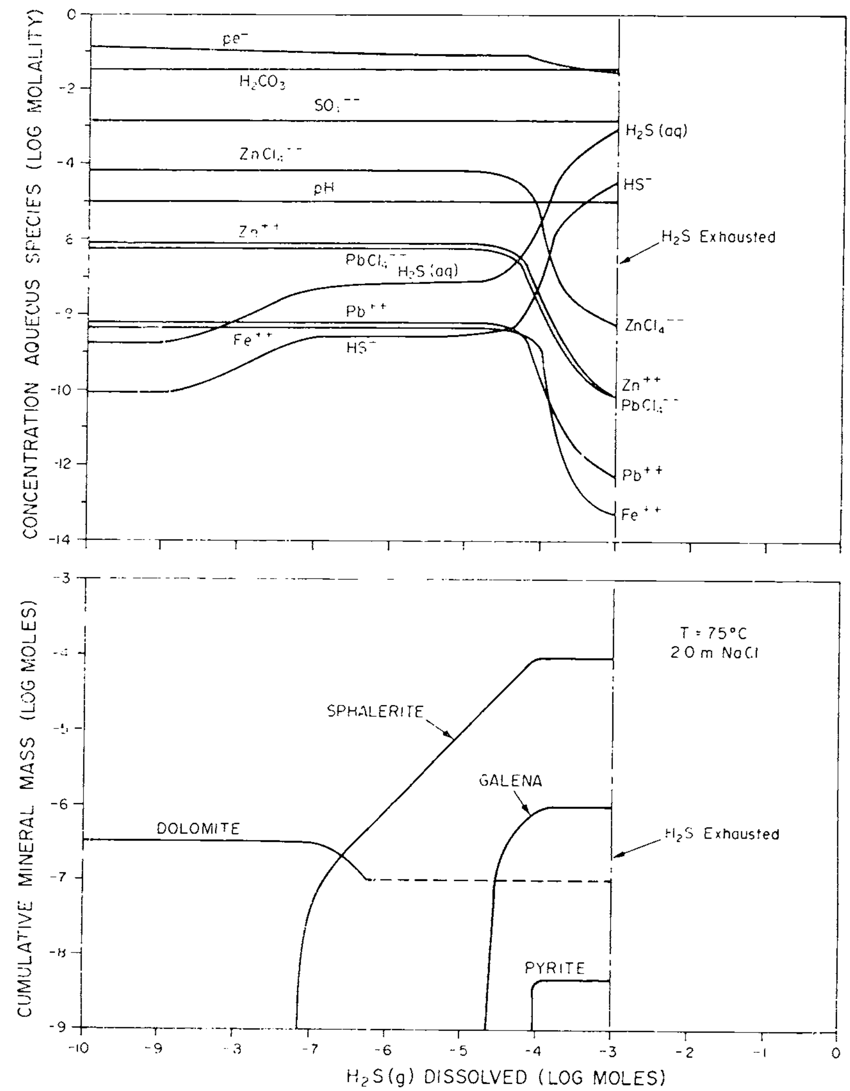

Fig. 22. EQ3/EQ6 simulation of the reaction of a metal-sulfate brine with hydrogen sulfide.

brine with H_2S resulted in about twenty-times more dolomite dissolution than the example of figure 22.

The addition of other strong reducing agents, such as methane or hydrogen gas, to a metal-bearing brine can also cause sulfide mineral precipitation. Methane is a common constituent of basinal brines, and fluid-inclusion data indicate that substantial amounts of CH_4 occurred in ore-forming fluids, possibly with concentrations as high as 800 mg/kg H_2O (Roedder, 1976). Dissolved methane may also reduce sulfate in brines internally, but the rate of reaction is thought to be too slow to be important in ore genesis (Barton, 1967). On the other hand, this process could allow CH_4 to be carried metastably in solution for long transport distances, perhaps to an ore-forming site where bacteria could enhance the reaction rate (Skinner, 1979).

The results of one simulation where methane is titrated into the metal-sulfate brine (table 7) are shown in figure 23. In this example 10^{-3} moles (16 mg) of CH_4 reacts with 1 kg of metal-bearing fluid at a temperature of 75°C. Addition of 10^{-7} moles of methane causes an abrupt drop in the oxidation state of the fluid, as marked by the pe$^-$ curve. The shift to a more reduced environment changes the sulfate to sulfide ratio which is reflected by the sudden increase in the $H_2S(aq)$ and HS^- concentrations. Dolomite was precipitated initially due to an over-saturation with respect to that phase, but as sphalerite begins to precipitate the dolomite slowly dissolves. As the fluid approaches equilibrium with respect to sphalerite, the addition of more CH_4 results in the deposition of galena and then pyrite. Sulfide precipitation ceases after about 10^{-4} moles of methane are dissolved, but further addition of methane results in a further drop of the oxidation state to more reduced conditions. At this stage large amounts of dolomite and calcite are precipitated, again because of sulfate reduction which in turn strongly influences carbonate equilibria. The process of late-stage carbonate mineralization is a common feature that is observed in many lead–zinc ore deposits. This process continues in the simulation, until the supply of CH_4 is exhausted. The same amounts of sulfide minerals precipitated here as in the H_2S model (fig. 22) but about 75 mg of calcite and 10 mg of dolomite are deposited per kg H_2O.

Another possible mechanism of reducing a sulfate-bearing brine is through replacement-type reactions with pre-existing sulfide minerals. Figure 24 considers the case where the model brine of table 7, containing 10^{-4} *m* Zn and 10^{-6} *m* Pb, passes through a pyrite-bearing carbonate bed. The amount of FeS_2 available for reaction per kg of fluid is 10^{-3} moles (120 mg). Compared with the preceding models, the reaction with pyrite appears to be a less efficient mechanism for ore precipitation, at least for these low metal concentrations. Only 10^{-6} moles (0.1 mg) of sphalerite precipitated in this reaction-path scenario before the fluid equilibrates with the pyrite. Subsequent simulations showed that greater amounts of ore will precipitate if the initial zinc and lead concentrations are much higher than those of figure 24. For example, assuming a zinc concentration of 10^{-3} moles/kg H_2O resulted in the precipitation of 38 mg of sphalerite per kg of fluid. Approx 2×10^{-4} moles (27 mg) of pyrite was destroyed in this simulation before the brine came into equilibrium with the pyrite phase.

All three reducing models given above have shown the viability of a metal-sulfate brine to produce ore mineralization at sites where H_2S is added to the fluid or the oxidation state is modified. Geologic evidence as to the relative importance of the various sulfate-reduction mechanisms

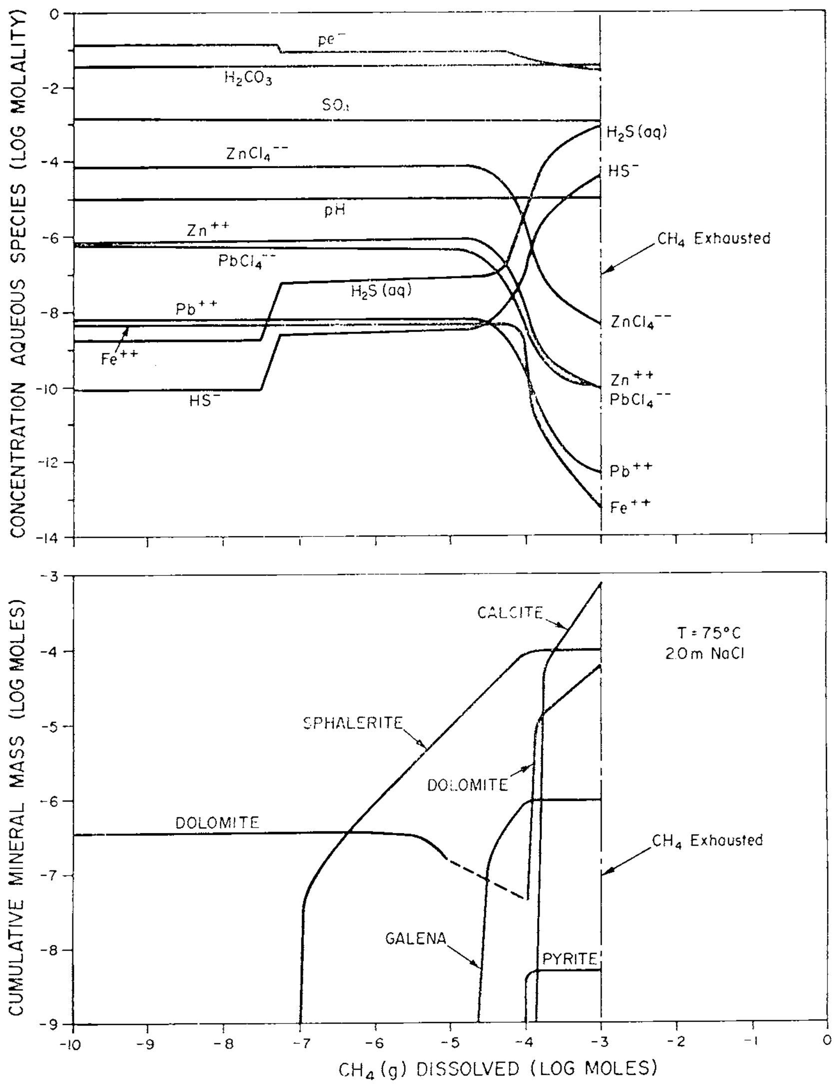

Fig. 23. EQ3/EQ6 simulation of the reaction of a metal-sulfate brine with methane.

has not been clearly established. It is known that bacteria-assisted sulfate reduction is unlikely in ore environments where temperatures are above 80°C; however, the inorganic mechanism suggested by Orr (1974) is apparently adequate for systems of 80° to 120°C in organic-rich strata. The fact remains that H_2S is abundant in the subsurface and is probably being continuously generated by several mechanisms under various temperature-depth conditions.

Metal-sulfide brine model.—We have seen that sulfate-reduction mechanisms allow a wide variety of geochemical conditions for the fluid

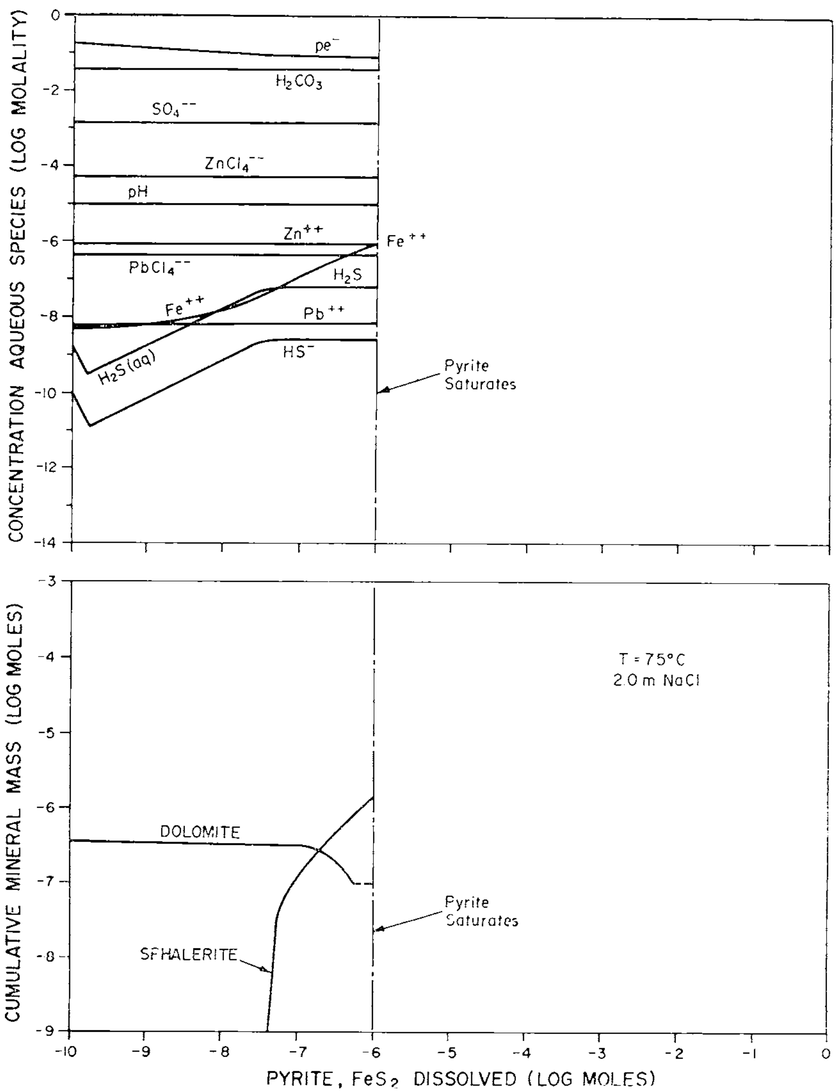

Fig. 24. EQ3/EQ6 simulation of the reaction of a metal-sulfate brine with pyrite.

transporting the metal to a depositional site. The geochemical conditions are much more restrictive in a brine transporting equilibrium amounts of both metal and aqueous sulfide, but a variety of precipitation mechanisms can still be called upon which will result in the deposition of sphalerite or galena from a metal-sulfide brine (table 6).

Simulation results are now presented to demonstrate the relative importance of two different precipitation scenarios for a metal-sulfide bearing brine. In the first simulation, the precipitation of sulfide minerals occurs when a metal-sulfide brine reacts with a dolomite bed. In the second simulation a drop in temperature causes ore precipitation from a brine that originally was in equilibrium with sphalerite, galena, and quartz.

Consider the model-brine composition of table 8. The solution is in equilibrium with quartz, sphalerite, and galena at a temperature of 100°C and oxidation state where $f_{O_2} = 10^{-55}$. Besides the mineral saturation constraints, higher temperature, and more reducing condition, the fluid is otherwise of similar element composition to the model brine of table 7. In this metal-sulfide brine, the sphalerite solubility produces a zinc concentration of 6.0×10^{-6} moles/kg H_2O in a 2.0 *m* NaCl solution. An equal amount of reduced sulfur is also present. Unlike previous simulations, the brine is undersaturated with respect to calcite and dolomite.

Figure 25 shows the results of one EQ3/EQ6 simulation in which the metal-sulfide brine (table 8) encounters a dolomite bed along its flow path. Approx 1 mole (185 g) of dolomite is allowed to react with 1 kg of the fluid. An increase in pH from 5.0 to 5.3 causes the brine to become

TABLE 8

$T = 100°C$
$pH = 5.0$
$f_{O_2} = 10^{-55}$ $f_{CO_2} = 5$ bars
(Eh = − 0.168 volts)

Component	Concentration totals (moles/kg)	Concentration totals (mg/kg)
Na	1.85	38,000
K	5.0×10^{-2}	1,745
Ca	5.0×10^{-2}	1,790
Mg	1.0×10^{-3}	20
SiO_2(aq)*	8.0×10^{-4}	20
Cl	2.0	63,330
SO_4	1.7×10^{-10}	1.5×10^{-5}
H_2CO_3(app)	2.8×10^{-2}	1,585
Fe	5.0×10^{-9}	2.5×10^{-6}
Zn**	6.0×10^{-6}	0.36
Pb†	1.0×10^{-7}	0.02
$S_{(r)}$††	6.0×10^{-6}	0.20

* Quartz saturation.
** Sphalerite saturation.
† Galena saturation.
†† Total reduced $sulfur_{(r)} = H_2S(aq) + HS^-$.

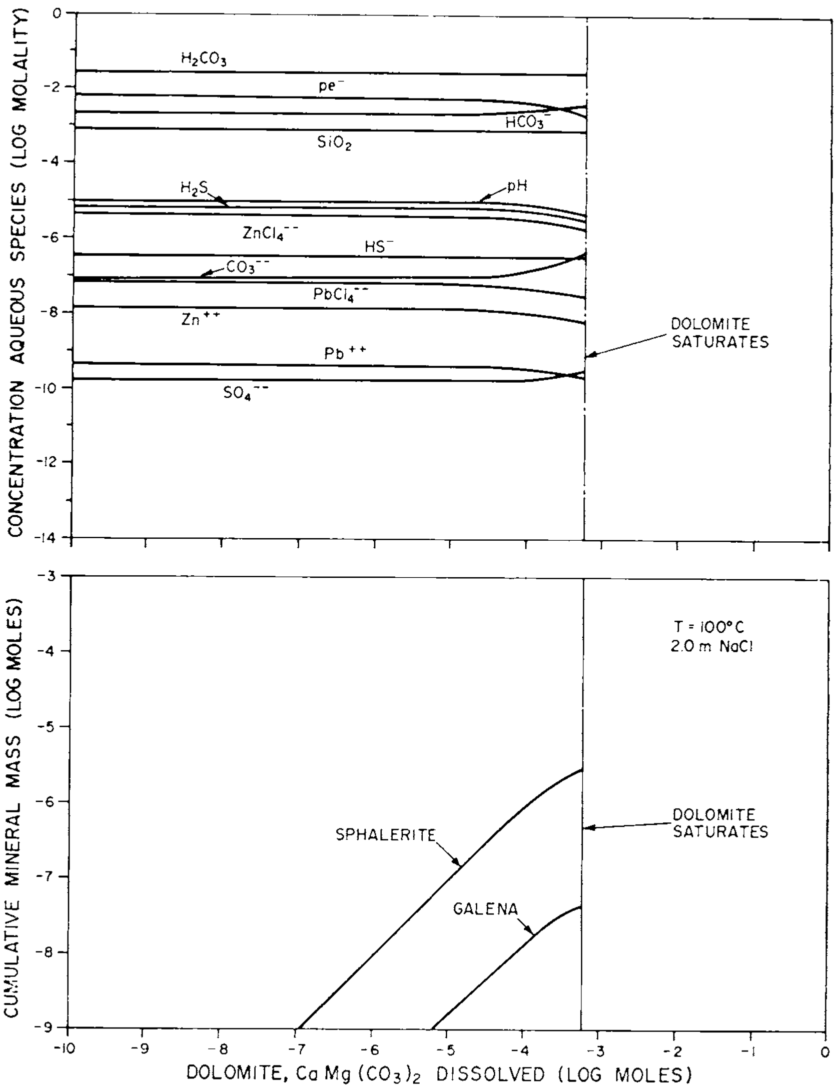

Fig. 25. EQ3/EQ6 simulation of the reaction of a metal-sulfide brine with dolomite.

saturated with respect to sphalerite first and then later with galena. This is accompanied by an increase in concentration of the carbonate-type aqueous species as the dolomite dissolves and a decrease in aqueous metal and sulfide concentrations as sphalerite and galena precipitate. The solution eventually becomes saturated with respect to dolomite, after about 6×10^{-4} moles (115 mg) have dissolved. The total mass of sphalerite precipitated is 3.1×10^{-6} moles (0.3 mg), and the total mass of galena precipitated is 4.6×10^{-8} moles (0.01 mg) both per kg H_2O.

Varying the salinity or temperature of the brine will naturally alter the solubility of sphalerite and galena, and therefore the expected amount of ore precipitation due to the pH shift. Several simulations were run where both salinity and temperature are varied over a salinity range of 1 to 6 *m* NaCl and temperature range of 25° to 150°C (Garven, ms). As expected, maximum deposition occurs from the most saline case (T = 100°C) in which 1×10^{-5} moles (1.1 mg) of sphalerite was deposited. Increasing the temperature from 100° to 150°C (at 2.0 *m* NaCl) resulted in a tenfold increase in the mass of sphalerite deposited to 3×10^{-5} moles (3 mg), again for a pH shift from 5.0 to 5.3. It is clear that high temperatures and salinities enable the metal-sulfide brine model to produce greater amounts of ore for a given pH change.

The second reaction mechanism to be tested is the effect of cooling. Figure 26 charts the mass-transfer results in which the model brine of table 8 is cooled from 100° to 60°C. The solution is initially saturated with respect to quartz, sphalerite, and galena. Over the 40°C temperature drop, about 5×10^{-6} moles (0.46 mg) of sphalerite, 9×10^{-8} moles (0.02 mg) of galena, and 5×10^{-4} moles (29.4 mg) of quartz are precipitated per kg H_2O. The temperature drop also caused the oxygen fugacity to vary from 10^{-55} to 10^{-65} bars, while the pH is slightly modified from 5.0 to 4.9. Precipitation of the secondary minerals forces an accompanying decrease in the concentration of most of the metal-chloride complexes, sulfide species, and aqueous silica. The change in temperature and oxidation state are effectively shifting the sulfate to sulfide ratio in the solution.

Within the first 10°C of cooling about 35 percent of the final mineral masses have precipitated. It takes roughly a 30°C drop in temperature to achieve a recovery of at least 85 percent of the sulfide minerals. Whether or not a cooling of 40°C is geologically reasonable is debatable. To localize enough ore through this amount of temperature change would require extremely high geothermal gradients. Based on the heat-transport modeling presented earlier, modest changes in temperature of 10°C are more likely to occur over short spatial intervals. The results of figure 26 indicate that even if large changes in temperature do occur, large flow rates and long periods of time are needed to form a major ore deposit by the cooling mechanism. Anderson (1975, 1977) and Sverjensky (1984) also evaluated the effect of pH shift and cooling on the precipitation of galena and sphalerite. Anderson's papers demonstrated that both processes can deposit appreciable quantities of metal if the brine is acidic. However, he doubts this acidity level occurs in basinal brines and concluded that transport of both metal and sulfide in the same fluid is not geologically important in the formation of Mississippi Valley-type deposits. On the other hand, Sverjensky, Rye, and Doe (1979) and Sverjensky (1981) noted that sulfur- and lead-isotope data from the Viburnum Trend of southeast Missouri support a transport model where sulfur is carried with metal to the site of deposition.

The results of this section suggest that the sulfide-type brine model may play a role in some ore districts. Large flow rates and long periods of mineralization would still be required if changes in pH and temperature are responsible for the precipitation. Long-distance transport of metal-sulfide solutions can be effectively ruled out as being important in stratabound ore genesis, unless both metal and sulfide are continually added to the fluid along the flow path. Otherwise, the effects of dispersion would dilute the already small equilibrium concentrations to even smaller amounts.

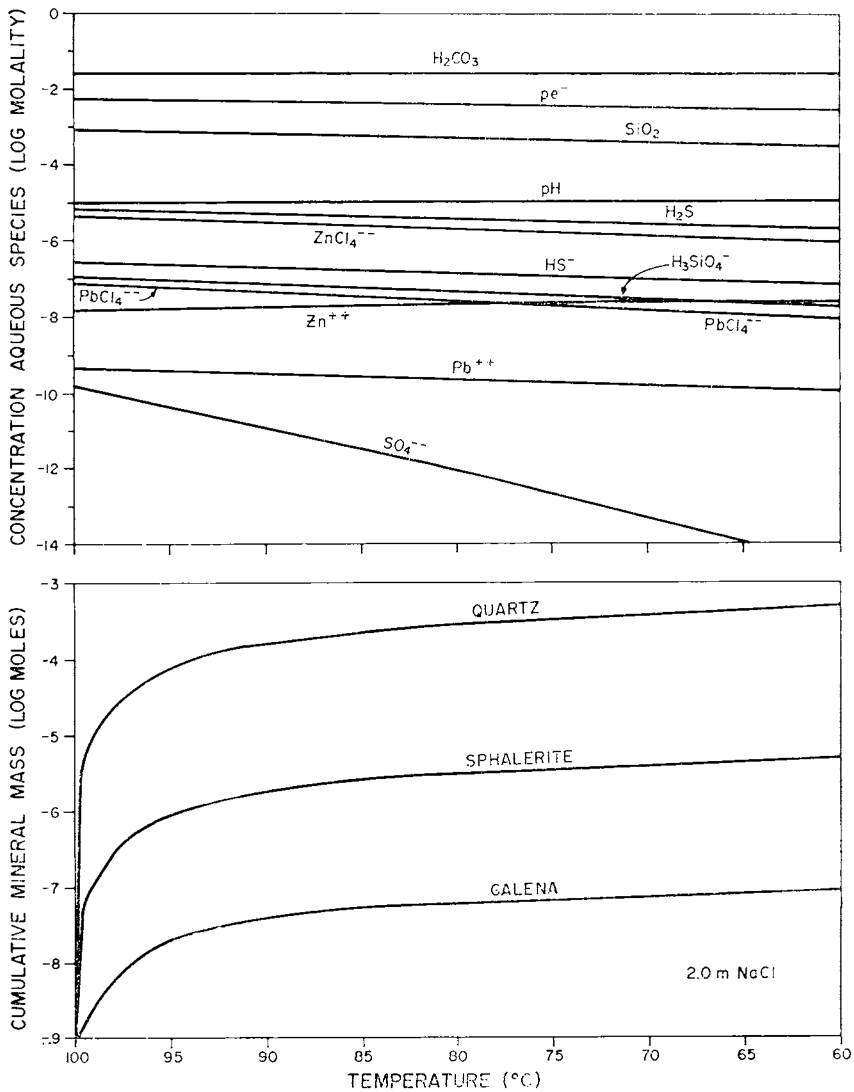

Fig. 26. EQ3/EQ6 simulation showing the effect of cooling a metal-sulfide brine from 100° to 60°C.

CONCLUSIONS

1. Mathematical modeling of transport processes in sedimentary basins can provide significant insight into the role of groundwater flow in stratabound ore formation. Although the mechanism of gravity-driven groundwater flow is not always favored in conceptual models of ore genesis, the quantitative results presented here suggest that it could be a principal agent in the formation of epigenetic, stratabound ore deposits. Modern analogs of the gravity-driven flow mechanism exist as regional flow systems in geologically mature basins throughout the world.

2. A generic simulation approach, where various types and sizes of hypothetical basins are modeled, is an effective way to study the factors affecting fluid flow, heat and mass transport, and geochemical mass transfer in gravity-driven flow systems. For this purpose, two-dimensional models of simplified geologic cross sections were found to be suitable. They allow one to perform a detailed sensitivity analysis of the transport parameters in a realistic manner, without resorting to a highly simplified one-dimensional model or costly numerical simulation of a basin in three dimensions.

3. The factors affecting steady-state fluid-flow patterns in sedimentary basins include the basin geometry, the water-table configuration, and the spatial variation in permeability. Fluid-flow rates depend largely on the hydraulic gradient imposed across the basin by the water-table slope and on the hydraulic properties of the strata, as well as fluid density and viscosity which are strongly affected by salinity and temperature gradients. Based on the results presented here, a gravity-driven groundwater system can sustain specific-discharge rates on the order of 1 to 10 m^3/m^2yr in extensive basin aquifers. Because of the variety of possible subsurface conditions, however, the range of feasible flow rates could be wider.

4. Under a gravity-drive system, groundwater flows from recharge areas in the elevated regions of a foreland basin to discharge areas in lower-elevation regions. The presence of layering in a basin results in the focusing of fluid flow down into the high-permeability unit in recharge areas and the focusing of flow upward and out of the unit in discharge areas. It is this focusing of groundwater flow that plays a key role in stratabound ore formation. The degree of focusing is controlled by the hydraulic conductivity contrast between the aquifer and surrounding strata. Contrast ratios as small as 10:1 are sufficient to permit significant cross-formational flow, thereby allowing for the natural transport of metal-bearing brines from shale source beds into regional aquifers over large areas of a basin.

5. Lateral variations in hydraulic conductivity can cause profound disruptions in a regional flow system, the effects of which in some cases can create local flow systems. This phenomenon commonly leads to the development of discharge areas in parts of a basin that otherwise would not have been expected from the classical image of the lateral-secretion hypothesis with discharge toward the basin margin. Local flow systems could also conceivably provide a transport mechanism for the gradual

supply of an ore-forming component such as sulfur into a metal-bearing brine flowing through a regional aquifer.

6. The length of a flow system in a basin depends on topographic relief, basin thickness, and permeability variations. If the basin is a few kilometers thick, if relief is gentle, and if an aquifer exists at depth, then continuous flow systems can develop over distances of several-hundred kilometers. In a wedge-shaped basin, fluid velocities in a basal aquifer are at a maximum near the shallow, downstream flank of the basin. Basement arches can restrict fluid flow to a thin stratigraphic interval, which will concentrate upward discharge and high flow rates above the arch. This feature may explain the association of some ore deposits with basement highs. Major river valleys can also interrupt regional flow paths by focusing fluid flow into the valley bottom. Paleotopography of the land surface and of the crystalline basement, therefore, can have an important influence on the location of ore formation through their control on flow systems.

7. Both conduction and convection are equally important heat-transport processes. Under conditions of very low fluid-flow rates, thermal conduction is the dominant form of heat transport. In a two-layer, 300-km long basin model with a hydraulic conductivity ratio between layers of 10:1 and an anisotropy ratio of 100:1 in both layers, the effects of thermal convection become visible in the temperature pattern when the hydraulic conductivity of the basal layer approaches a value of 10 m/yr. The amount of convection in a basin is determined by the hydrodynamics, and, therefore, all the factors that affect fluid flow also affect subsurface temperatures.

8. The existence of gravity-driven groundwater flow systems results in the lowering of temperatures in recharge areas and the elevation of temperatures in discharge areas of a sedimentary basin, with respect to the thermal regime expected for conduction alone. The differing gradients are caused by the convection of heat away from the deeper parts of the basin and updip to the discharge area of the regional fluid-flow system near the basin margin. Depending on the hydraulic conductivity and its anisotropy, the temperature can be raised as much as 30°C in discharge areas, over the temperature expected under conduction alone. Groundwater discharge zones, whether they are caused by permeability pinchouts, topographic expressions, or basement arches, can significantly perturb the regional temperature pattern. It is possible that the high geothermal gradients created by these features could play a role in localizing ore precipitation through cooling.

9. On the basis of the effects of their thermal conductivities on heat and fluid-flow patterns, the presence of overlying sequences of shale and limestone is conducive to the development of temperatures in a basal aquifer that are characteristic of ore-forming environments.

10. Thermal dispersion has a weak influence on the temperature pattern in a basin. The main role of this parameter is probably its ability to damp out thermal instabilities related to free convection.

11. Based on the representative range of continental heat flows of 50 to 80 mW/m^2 and surface temperatures of 10° to 30°C, maximum temperatures near the shallow edge of a 300-km long, wedge-shaped basin can range from about 50° to 95°C at a depth of less than 1000 m. Temperatures of 100° to 150°C are possible in larger basins with dimensions of several kilometers in maximum thickness by several-hundred kilometers in lateral extent. There is no need, therefore, to invoke deep-seated heat sources to explain the occurrence of warm temperatures at shallow depths in stratabound ore formation.

12. Mass transport in basinal flow systems occurs by the combined processes of advection, dispersion, diffusion, and geochemical mass transfer. In the absence of hydrodynamic dispersion and chemical reactions along the flow path between source beds and depositional sites, the transport of aqueous metal is solely governed by the fluid-flow regime, and mass that is released from a source bed will travel as an undisturbed plug along the flowline with the average linear velocity of the groundwater. The focusing of fluid flow through an aquifer results in a focusing of mass because of advective transport, and therefore it is critical to the occurrence or non-occurrence of ore-forming conditions in a basin.

13. Hydrodynamic dispersion includes the processes of mechanical dispersion and molecular diffusion. Mechanical dispersion is a mixing process that results in the spreading of an ore-forming constituent in both a longitudinal and transverse direction with respect to the flow path. Diffusion in a porous medium also results in the reduction of concentration gradients, but its effects are usually several orders of magnitude smaller than mechanical dispersion. The effects of dispersion are in a direction counter to those favorable for the concentration of mass in ore deposits. The formation of ore deposits is most likely to occur in systems of low dispersivity.

14. In many cases the influence of dispersion on long-distance transport of metals can be severe. For transport distances of 300 km, dispersion can dilute the metal concentration of the brine to a value that is 10 to 20 percent of the source-bed concentration. For such a basin, if 1 mg/kg H_2O is taken as the minimum metal concentration needed to produce a major ore body, then approx 5 to 10 mg/kg H_2O must be present originally in the source-bed area, assuming there are no other sources or sinks for the metal along the flow path.

15. A variety of geologic and water-table configurations can create local flow systems that lead to the convergence of regional flow paths from different stratigraphic levels. But it is unlikely that mixing of two chemically-distinct fluids would occur over a small-enough area to localize an ore deposit, unless at the local level flow is being restricted to fracture zones or solution channels.

16. The main factors affecting the solubilities of galena and sphalerite in basinal brines include the temperature, the salinity, and the pH and oxidation state. Metal concentrations of several tens of mg/kg H_2O are theoretically possible, provided the sulfide content of the brine is very

low. Sulfide can be supplied at the ore-forming site, either through reduction of sulfate in the metal-bearing brine or by addition of H_2S through reactions with the surrounding rocks. Other reducing agents such as methane or pre-existing iron-sulfide minerals can also cause ore deposition.

17. Metal and aqueous sulfide can be transported in the same fluid at equilibrium, but a combination of high salinity, high temperature, and acidic conditions (pH = 3-5) is required to achieve concentrations of even a few mg/kg H_2O. Precipitation of ore can be accomplished through a pH shift or cooling. The pH change is usually assumed to come from the dissolution of carbonates. However, neither of these mechanisms is very effective at depositing sulfides when the pH is greater than 5.0 and the temperature is less than 80°C, and the salinity is below 3 *m* NaCl. Furthermore, a rather narrow range of pH and oxygen fugacity conditions restrict the possible composition range of equilibrium solutions carrying metal and sulfide through carbonate rocks.

18. The relative importance of these two geochemical models may vary from one basin environment to another. Geologic evidence from some ore districts indicates a sulfate-reducing mechanism for ore precipitation, while other districts support a model with simultaneous transport of metal and sulfide.

19. Long-distance transport (100-300 km) of metal and sulfide in solution can probably be ruled out because the dilution effect of dispersion would have reduced these small concentrations even lower. Continuous addition of both metal and sulfide along the flow path or perhaps much higher initial concentrations due to organic complexing may overcome the dilution problem. However, large flow rates and long periods of time would still be required if changes in pH and temperature are responsible for ore deposition. The transport of metal and sulfate together is a more defensible mechanism, both with respect to geochemistry and hydrodynamics.

20. This study has shown that gravity-driven flow systems are capable of forming favorable conditions for the genesis of large ore deposits over reasonably short intervals of geologic time. Numerical modeling provides a powerful research tool for testing ore-genesis hypotheses and for developing an understanding of the conditions necessary for ore deposition in sedimentary basins. Because of the generic nature of the modeling, the results presented here should also give general insight to other geologic processes involving fluid-flow in sedimentary basins, especially in regard to problems of sediment diagenesis and petroleum migration and accumulation. It is hoped that the theoretical work begun in this study will encourage future hydrogeologic research in these fields, as well as continued analysis of ore genesis.

ACKNOWLEDGMENTS

This research was supported by a grant to Allan Freeze from the Natural Sciences and Engineering Research Council of Canada. Completion of the study was aided by additional funding for computer time from the University of British Columbia. We are very grateful to Thomas Wolery of the Lawrence Livermore Laboratory for providing access to his geochemical codes. We particularly want to thank Tom Brown for steering our analysis to include water/rock geochemistry and for his advice and instruction in the subject of geochemical modeling. Leslie Smith aided our work by sharing with us his expertise on transport modeling and by his day-to-day interest on the modeling study progress. The authors also benefited from the interest and helpful discussions provided by Ghislain de Marsily, Denis Norton, and Jack Sharp.

References

Anderson, G. M., 1973, The hydrothermal transport and deposition of galena and sphalerite near 100°C: Econ. Geology, v. 69, p. 480-482.

——— 1975, Precipitation of Mississippi Valley-type ores: Econ. Geology, v. 70, p. 937-942.

——— 1977, Thermodynamics and sulfide solubilities, *in* Greenwood, H. J., ed., Short course in application of thermodynamics to petrology and ore deposits: Vancouver, Mineralog. Assoc. Canada, p. 136-150.

——— 1978, Basinal brines and Mississippi Valley-type ores: Episodes, v. 1978, p. 15-19.

Anderson, G. M., and Macqueen, R. W., 1982, Ore deposit models — 6 Mississippi Valley-type lead–zinc deposits: Geosci. Canada, v. 9, p. 108-117.

Anderson, M. P., 1979, Using models to simulate the movement of contaminants through groundwater flow systems: Chemical Rubber Co., Critical Reviews in Environmental Control, v. 9, p. 97-156.

Barnes, H. L., and Czamanske, G. K., 1967, Solubilities and transport of ore minerals, *in* Barnes, H. L., ed., Geochemistry of Hydrothermal Ore Deposits, 1st ed.: New York, Holt, Rinehart and Winston, p. 334-381.

Barrett, T. J., and Anderson, G. M., 1982, The solubility of sphalerite and galena in NaCl brines: Econ. Geology, v. 77, p. 1923-1933.

Barton, P. B., Jr., 1967, Possible role of organic matter in the precipitation of the Mississippi Valley ores: Econ. Geology, Mon. 3, p. 371-378.

Betcher, R. N., ms, 1977, Temperature distribution in deep groundwater flow systems — a finite element model: M.Sc. thesis, Univ. of Waterloo, Waterloo, Ontario.

Billings, G. K., Kesler, S. E., and Jackson, S. A., 1969, Relation of zinc-rich formation waters, northern Alberta, to the Pine Point ore deposit: Econ. Geology, v. 64, p. 385-391.

Bischoff, J. L., Radtke, A. S., and Rosenbauer, R. J., 1981, Hydrothermal alteration of graywacke by brine and seawater: Roles of alteration and chloride complexing on metal solubilization at 200°C and 350°C: Econ. Geology, v. 76, p. 676-695.

Bond, D. C., 1972, Hydrodynamics in deep aquifers of the Illinois basin: Urbana, Ill., Illinois State Geol. Survey, Circ. 470, 51 p.

Brace, W. F., 1980, Permeability of crystalline and argillaceous rocks: Internat. Jour. Rock Mechanics and Mining Sci., v. 17, p. 241-251.

Bredehoeft, J. D., Blyth, C. R., White, W. A., and Maxey, G. B., 1963, Possible mechanism for concentration of brines in subsurface formations: Am. Assoc. Petroleum Geologists Bull., v. 47, p. 257-269.

Bredehoeft, J. D., and Papadopoulos, I. S., 1965, Rates of vertical groundwater movement estimates from the Earth's thermal profile: Water Resources Research, v. 1, p. 325-328.

Brown, A. C., 1971, Zoning in the White Pine copper deposit. Ontonagon County, Michigan: Econ. Geology, v. 66, p. 543-573.

Carpenter, A. B., Trout, M. L., and Pickett, E. E., 1974, Preliminary report on the origin and evolution of lead- and zinc-rich oil field brines in central Mississippi: Econ. Geology, v. 69, p. 1191-1206.

Clark, S. P., Jr., 1966, Thermal conductivity, *in* Clark, S. P., Jr., ed., Handbook of Physical Constants: Geol. Soc. America Mem. 97, sec. 21, p. 459-473.

Davis, S. N., 1969, Porosity and permeability of natural materials, *in* De Wiest, R. J. M., ed., Flow Through Porous Media: New York, Academic Press, p. 54-89.

Domenico, P. A., and Palciauskas, V. V., 1973, Theoretical analysis of forced convective heat transfer in regional groundwater flow: Geol. Soc. America Bull., v. 84, p. 3803-3814.

Ellis, A. J., 1968, Natural hydrothermal systems and experimental hot water/rock interaction: reactions with NaCl solutions and trace metal extraction: Geochim. et Cosmochim. Acta, v. 32, p. 1313-1363.

Freeze, R. A., and Cherry, J. A., 1979, Groundwater: Englewood Cliffs, N.J., Prentice-Hall, Inc., 604 p.

Freeze, R. A., and Witherspoon, P. A., 1966, Theoretical analysis of regional groundwater flow: 1. Analytical and numerical solutions to the mathematical model: Water Resources Research, v. 2, p. 641-656.

——— 1967, Theoretical analysis of regional groundwater flow: 2. Effect of water-table configuration and subsurface permeability variation: Water Resources Research, v. 3, p. 623-634.

——— 1968, Theoretical analysis of regional groundwater flow: 3. Quantitative interpretations: Water Resources Research, v. 4, p. 581-590.

Garven, Grant, ms, 1982, The role of groundwater flow in the genesis of stratabound ore deposits: A quantitative analysis: Ph.D. dissert., Univ. of British Columbia, Vancouver, Canada, 304 p.

Garven, G., and Freeze, R. A., 1984, Theoretical analysis of the role of groundwater flow in the genesis of stratabound ore deposits: 1. Mathematical and numerical model: Am. Jour. Sci., v. 284, p. 1085-1124.

Giordana, T. H., and Barnes, H. L., 1981, Lead transport in Mississippi Valley-type ore solutions: Econ. Geology, v. 76, p. 2200-2211.

Helgeson, H. C., 1964, Complexing and Hydrothermal Ore Deposition: New York, Pergamon Press, Inc., 128 p.

——— 1969, Thermodynamics of hydrothermal systems at elevated temperatures and pressures: Am. Jour. Sci., v. 267, p. 729-804.

Hitchon, B., 1969a, Fluid flow in the Western Canada sedimentary basin: 1. Effect of topography: Water Resources Research, v. 5, p. 186-195.

——— 1969b, Fluid flow in the Western Canada sedimentary basin: 2: Effect of geology: Water Resources Research, v. 5, p. 460-469.

——— 1976, Hydrogeochemical aspects of mineral deposits in sedimentary rocks, *in* Wolf, K. H., ed., Handbook of Strata-Bound and Stratiform Ore Deposits: New York, Elsevier, v. 2, p. 53-66.

——— 1977, Geochemical links between oil fields and ore deposits in sedimentary rocks, *in* Garrard, P., ed., Proceedings of the forum on oil and ore in sediments: London, England, Imperial College, Dept. Geology, p. 1-37.

——— 1981, Genetic links between shales, formation fluids and ore deposits-example for zinc from Alberta, Canada [abs.]: Geol. Soc. America Abs. with Programs, v. 13, no. 7, p. 473.

Hitchon, B., Billings, G. K., and Kovan, J. E., 1971, Geochemistry and origin of formation waters in the Western Canada sedimentary basin: III. Factors controlling chemical composition: Geochim. et Cosmochim. Acta, v. 35, p. 567-598.

Jessop, A. M., and Lewis, T. L., 1978, Heat flow and heat generation in the Superior Province of the Canadian Shield: Tectonophysics, v. 50, p. 55-77.

Kappelmeyer, O., and Haenal, R., 1974, Geothermics — with Special Reference to Application: Berlin-Stuttgart, Borntraeger.

Kimbell, C. L., 1979, Hydrogen sulfide measurement in geothermal wells: Geothermal Resources Council Trans., v. 3, p. 333-335.

Land, L. S., and Prezbindowski, D. R., 1981, The origin and evolution of saline formation water, Lower Cretaceous carbonates, southcentral Texas, U.S.A.: Jour. Hydrology, v. 54, p. 51-74.

Orr, W. L., 1974, Changes in sulfur content and isotopic ratios of sulfur during petroleum maturation — study of Big Horn Paleozoic oils: Am. Assoc. Petroleum Geologists Bull., v. 50, p. 2295-2318.

Parsons, M. L., 1970, Groundwater thermal regime in a glacial complex: Water Resources Research, v. 6, p. 1701-1720.

Pickens, J. F., and Lennox, W. C., 1976, Numerical simulation of waste movement in steady groundwater flow systems: Water Resources Research, v. 12, p. 171-180.

Roedder, E., 1967, Environment of deposition of stratiform (Mississippi Valley-type) ore deposits, from studies of fluid inclusions: Econ. Geology Mon. 3, p. 349-362.

——— 1976, Fluid inclusion evidence in the genesis of ores in sedimentary and volcanic rocks, *in* Wolf, K. H., ed., Handbook of Strata-Bound and Stratiform Ore Deposits: New York, Elsevier, v. 4, p. 67-110.

Rubin, H., 1974, Heat dispersion effect on thermal convection in a porous medium layer: Jour. Hydrology, v. 21, p. 173-185.

Sass, J. H., Blackwell, D. D., Chapman, D. S., Costain, J. K., Decker, E. R., Lawver, L. A., and Swanberg, C. A., 1981, Heat flow from the crust of the United States, *in* Touloukian, Y. S., Judd, W. R., and Roy, R. F., eds., Physical Properties of Rocks and Minerals: New York, McGraw-Hill, p. 503-548.

Schwartz, F. W., 1977, Macroscopic dispersion in porous media: The controlling factors: Water Resources Research, v. 13, p. 743-752.

Skinner, B. J., 1979, The many origins of hydrothermal mineral deposits, *in* Barnes, H. L., ed., Geochemistry of Hydrothermal Ore Deposits, 2d ed.: New York, John Wiley & Sons, Inc., p. 1-21.

Smith, L., and Chapman, D. S., 1983, On the thermal effects of groundwater flow: 1. Regional scale systems: Jour. Geophys. Research, v. 88, p. 593-608.

Stallman, R. W., 1963, Computation of groundwater velocity from temperature data, *in* Bentall, R., ed., Methods of collecting and interpreting groundwater data: U.S. Geol. Survey, Water Supply Paper 1554-H, p. 36-46.

Sverjensky, D. A., 1981, The origin of a Mississippi Valley-type deposit in the Viburnum trend, southeast Missouri: Econ. Geology, v. 76, p. 1848-1872.

———— 1984, Oil-field brines as ore-forming solutions: Econ. Geology, v. 79, p. 23-37.

Sverjensky, D. A., Rye, D. M., and Doe, B. R., 1979, The lead and sulfur isotopic compositions on galena from a Mississippi Valley-type deposit in the New Lead Belt, southeast Missouri: Econ. Geology, v. 74, p. 149-153.

Tóth, J., 1962, A theory of groundwater motion in small drainage basins in central Alberta: Jour. Geophys. Research, v. 67, p. 4375-4387.

———— 1963, A theoretical analysis of groundwater flow in small drainage basins: Jour. Geophys. Research, v. 68, p. 4795-4812.

———— 1978, Gravity-induced cross-formational flow of formational fluids, Red Earth region, Alberta, Canada: Analysis, patterns, and evolution: Water Resources Research, v. 14, p. 805-843.

Tyvand, P. A., 1977, Heat dispersion effect on thermal convection in anisotropic porous media: Jour. Hydrology, v. 34, p. 335-342.

van Everdingen, R. O., 1968, Studies of formation waters in Western Canada: Geochemistry and hydrodynamics: Canadian Jour. Earth Sci., v. 5, p. 523-543.

Weber, J. E., 1975, Dispersion effect on buoyancy-driven convection in stratified flows through porous media: Jour. Hydrology, v. 25, p. 59-70.

White, D. E., 1968, Environments of generation of some base-metal ore deposits: Econ. Geology, v. 63, p. 301-335.

White, W. S., 1971, A paleohydrologic model for mineralization of the White Pine copper deposit, northern Michigan: Econ. Geology, v. 66, p. 1-13.